Supporting Information

Structure-guided Evolution of a Ketoreductase for Efficient and Stereoselective Bioreduction of Bulky α-Amino β-Keto Esters

Jiawei Tang,[†,#] Liuqing Chen,[§,#] Luwen Zhang,[‡] Guowei Ni,[‡] Jun Yu,[‡] Hongyi Wang,[‡] Fuli Zhang,[‡] Shuguang Yuan,[§,*] Meiqing Feng,[†,*] and Shaoxin Chen,[‡,*]

†Department of Biological Medicines & Shanghai Engineering Research Center of Immunotherapeutics, Fudan University School of Pharmacy, Shanghai 201203, P. R. China

‡Shanghai Institute of Pharmaceutical Industry, China State Institute of Pharmaceutical Industry, 285 Gebaini Road, Pudong, Shanghai 201203, P. R. China

§Shenzhen Institutes of Advanced Technology, Chinese Academy of Sciences, Shenzhen 518055, P. R. China

Table of contents

1. Compounds preparation and characterization

1.1 Synthesis of methyl 2-[(tert-butoxycarbonyl) amino]-3-[4-(nitro)-phenyl]-3-oxopropanoate (5a)

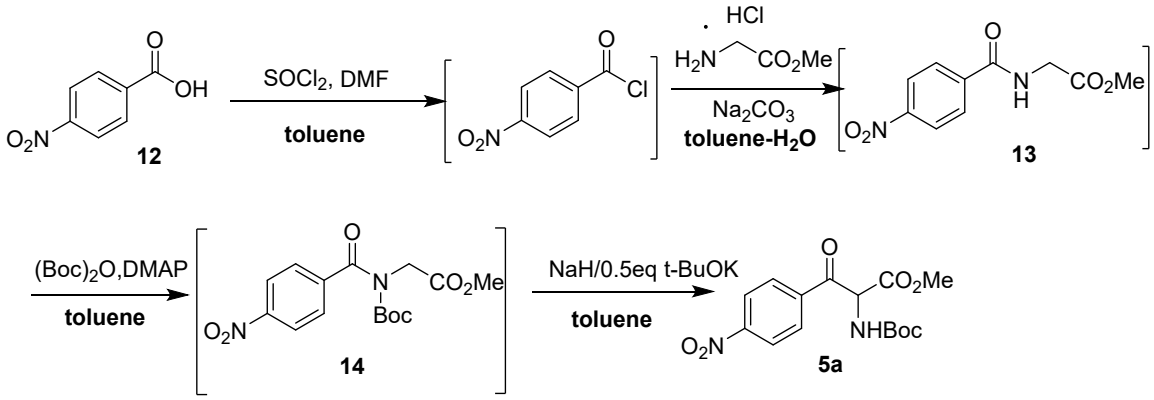

To a stirred solution of 4-nitrobenzoic acid (100 g, 0.60 mol) in dimethylformamide (DMF) (10 mL) and toluene (500 mL) was added $SOCl_2$ (90 g) over 1 h, maintaining the internal temperature below 10℃. The reaction temperature was then warmed to 60℃, and the reaction was stirred for 5 h. When the reaction was completed, the stirred solution was distilled under vacuum to afford 4-nitrobenzoyl chloride for the next step directly.

To a stirred solution of glycine methyl ester hydrochloride (90 g, 0.72 mol) in H_2O (500 mL) and toluene (500 mL), an aqueous solution of Na_2CO_3 (82 g, 0.77 mol) was added dropwise below 10℃. The mixture was kept for 0.5 h at room temperature. Then the solution of 4-nitrobenzoyl chloride in toluene (500 mL) was added and stirred for 4 h. The reaction was monitored by LC-MS and terminated when the conversion reached 98%. Then, the reaction was filtrated for partial solid and extracted with toluene (200 mL×2). The layers were separated, and the organic layer was washed with an aqueous saturated NaCl solution. The solution was distilled under vacuum to yield the off-white solid. The product was dried for the next step.

To a stirred solution of the above solid in toluene (1000 mL), 4-dimethylaminopyridine (DMAP) (6 g, 0.049 mol) was charged in one potion. $(Boc)_2O$ (156.8 g, 0.72 mmol) was added slowly below 10 ℃. The reaction was stirred for 5 h at 25℃. Then the solvent was evaporated under vacuum to afford white solid **14**, which was used for the next step directly.

To a stirred solution of sodium hydride (35.9 g, 60% content, 0.90 mol) and *t*-BuOK (33.5 g, 0.30 mol) in toluene (500 mL) under N_2 atmosphere was added dropwise. The solution of the above step product in toluene (500 mL) was added dropwise at -5~0℃. The mixture was stirred for 5 h. Then, the precooling solution of acetic acid (50%) in toluene was added to adjust the pH to 7.0-7.5. The reaction was quenched by H_2O (1000 mL) and extracted with EtOAc (300 mL×2). Then, the combined organic phase was dried with Na_2SO_4. The filtrate was concentrated under vacuum to yield the target compound **5a** (156.6 g) as a light-yellow solid. ^{1}H NMR (600 MHz, $CDCl_3$) δ 8.35 (d, J = 8.8 Hz, 2H), 8.27 (d, J = 8.8 Hz, 2H), 5.96 (d, J = 7.9

Hz, 1H), 5.86 (d, *J* = 7.7 Hz, 1H), 3.75 (s, 3H), 1.45 (s, 9H). ^{13}C NMR (151 MHz, $CDCl_3$) δ 191.30, 166.85, 154.89, 150.83, 138.92, 130.44, 123.91, 81.19, 59.45, 53.46, 28.19.

1.2 Synthesis of ethyl 2-[(tert-butoxycarbonyl) amino]-3-[4-(methylsulfonyl)-phenyl]-3-oxopropanoate (7a)

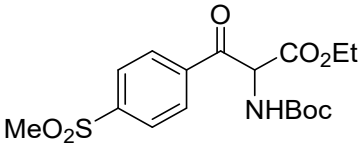

Compound (**7a**) was prepared by an analogous manner[1]. ^{1}H NMR (400 MHz, $CDCl_3$): δ 8.26(d, *J*=8 Hz,2H), 8.07(d, *J*=8 Hz,2H), 5.93-5.86 (m, 2H),4.21-4.15(m, 2H),3.08(s, 3H),1.43(s, 9H),1.16(t, *J*=7.2 Hz, 3H); ^{13}C NMR (150 MHz, CD_3OD): δ 191.8, 166.4, 155.1, 145.1, 138.7, 130.3, 127.9, 81.1, 62.9, 59.8, 44.3, 28.3, 14.0.

1.3 Synthesis of methyl 2-[(tert-butoxycarbonyl)amino]-3-[4-(methylsulfonyl)-phenyl]-3-oxopropanoate (8a)

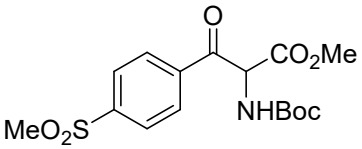

The compound (**8a**) was prepared by the same procedure[1]. ^{1}H NMR (600 MHz, $CDCl_3$): *δ* = 8.28 (d, *J* = 8.22 Hz, 2 H),8.09 (d, *J* = 8.34 Hz, 2 H), 5.96 (d, *J* = 7.92 Hz, 1 H), 5.87 (d, *J* =7.62 Hz, 1 H), 3.75 (s, 3 H), 3.10 (s, 3 H), 3.27 (s, 1 H), 1.45 (s, 9H) ppm. ^{13}C NMR (150 MHz, $CDCl_3$): *δ* = 191.53, 166.90, 154.92,145.04, 138.44, 130.23, 127.89, 81.15, 59.37, 53.46, 44.27, 28.21.

1.4 Synthesis of (2*S*,3*R*)-5b

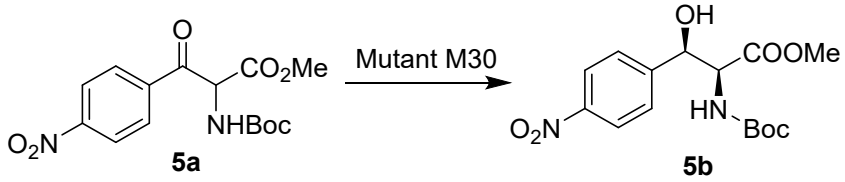

Glucose (32 g), mutant M30 wet cells (40 g), GDH (10 g), and $NADP^+$ (0.1 g) were added to a stirred solution of phosphate buffer (pH 7.0, 100 mL). Then the compound **5a** (20 g) and DMSO (100 mL) were added to the above mixture. The reaction was carried out at 30°C and stirred mechanically for 24 h. During the reaction, the pH value was kept at 7.0 by titrating the 5% Na_2CO_3 solution. After the reaction was completed, the mixture was extracted with methyl tert-butyl ether three times (250 mL×3). The organic phase was combined, dried over anhydrous Na_2SO_4, and evaporated under vacuum. Finally, the product **(2*S*, 3*R*)-5b** was dried at 50°C, yielding 17.1 g of light-yellow solid (chemical purity 97.1%, chiral purity *ee*>99.9%, *de* 99.9%). Chiral HPLC is shown in Table S4. The identity of the product was confirmed using ^{1}H and ^{13}C NMR. ^{1}H NMR (600 MHz, $CDCl_3$) δ 8.17 (t, *J* = 12.8 Hz, 2H), 7.54 (t, *J* = 12.8

Hz, 2H), 5.36 (t, *J* = 12.7 Hz, 2H), 4.57 (d, *J* = 8.1 Hz, 1H), 3.78 (s, 3H), 3.53 (s, 1H), 1.26 (d, *J* = 17.0 Hz, 9H). ^{13}C NMR (151 MHz, $CDCl_3$) δ 170.82, 147.54, 147.31, 127.05, 123.45, 80.56, 77.28, 77.07, 76.85, 73.06, 59.16, 52.87, 28.26, 28.08.

1.5 Synthesis of chloramphenicol

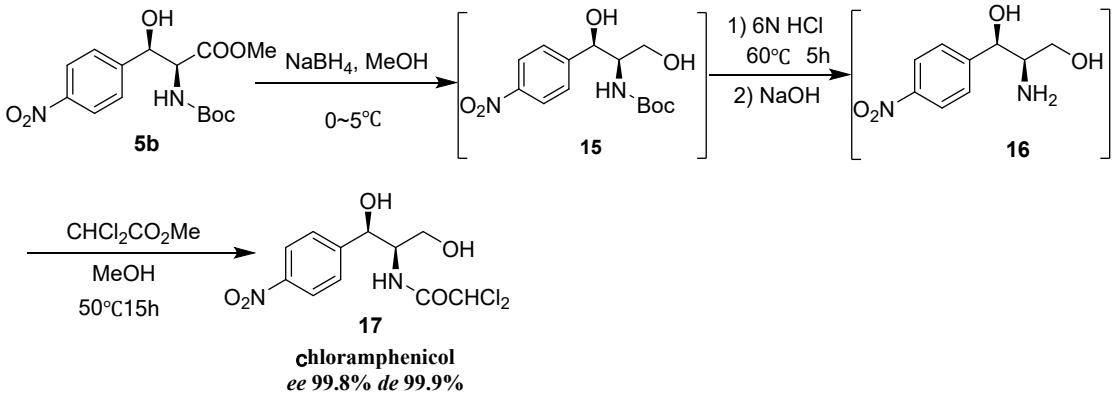

(2*S*, 3*R*)-5b (15 g) was dissolved in methanol (30 mL) and stirred at 0~5 ℃. $NaBH_4$ was added in portions (3 g), and then the mixture was stirred for 2 h. The reaction was monitored by LC-MS. Subsequently, the aqueous HCl (6 N, 15 mL) was added to the resulting solution, and the mixture was stirred at 60 ℃ for 5 h. After the reaction was completed, the pH was adjusted to 7-8 by 30% NaOH and then concentrated to afford the off-white solid with MeOH (the water content was controlled below <0.5%). The solid was dissolved in MeOH (100 mL). After filtration, dichloroacetic acid methyl ester (7.7 g) was added to the filtrate, and the mixture was stirred at 50 ℃ for 15 h. When the reaction was completed, the solvent MeOH was removed under reduced pressure. The reaction was quenched by adding H_2O (100 mL) and EtOAc (100 mL). The aqueous phase was extracted with EtOAc (100 mL×2). The combined organic phase was washed with brine (30 mL×2) and dried with Na_2SO_4. The organic phase was filtrated and concentrated to afford the white solid. The crude product was recrystallized with MeOH/H_2O (*v/v* 1/3). Finally, 12.1 g of product **17** was obtained as white crystals, chemical purity 99.3%, chiral purity *ee* 99.8%, *de* 99.9%. m.p.148.8~149.2℃ ^{1}HNMR (600 MHz, CD_3OD) δ 8.21 – 8.18 (m, 2H), 7.66 (d, *J* = 8.5Hz, 2H), 6.25 (s, 1H), 5.18 (d, *J* = 2.6 Hz, 1H), 4.16 (td, *J* = 7.1, 2.7Hz, 1H), 3.83 (dd, *J* = 10.9, 7.2 Hz, 1H), 3.63 (dd, *J* = 10.9, 6.1 Hz,1H), 3.33 (dt, *J* = 3.2, 1.6 Hz, 1H), ^{13}CNMR (151 MHz, CD_3OD) δ 166.57, 151.65, 148.59, 128.33, 124.16, 71.26, 67.36, 62.21, 58.50, 49.42, 49.28, 49.14, 49.00, 48.86, 48.72, 48.58. HRMS: calcd. for $C_{11}H_{13}Cl_2N_2O_5$ [M+H] 323.0194 found 323.0196. Chiral chromatographic condition: Chiralpak OD-3(4.6×250 mm, 3 μm, DACEL, shanghai), mobile phase: 90% n-hexane (0.1%TFA)/10% i-PrOH, 254 nm, 0.8 mL/min, 30℃, t_R=12.3 min for the chloramphenicol.

1.6 Synthesis of 1b-4b and 6b-11b

1b-4b and **6b-11b** was respectively prepared from **1a-4a** and **6a -11a,** according to the synthesis method of **5b**.

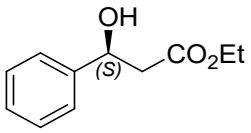

1b

Chiral HPLC method is show in Table S4. $[\alpha]_D^{28}$ = -50.4° (*c* 0.25, Chloroform). ^{1}H NMR (600 MHz, $CDCl_3$) δ 7.40 – 7.33 (m, 4H), 7.29 (ddd, *J* = 6.2, 3.1, 1.5 Hz, 1H), 5.13 (dd, *J* = 9.2, 3.7 Hz, 1H), 4.17 (q, *J* = 7.1 Hz, 2H), 3.54 (s, 1H), 2.73 (ddd, *J* = 20.0, 16.2, 6.5 Hz, 2H), 1.26 (t, *J* = 7.2 Hz, 3H). ^{13}C NMR (151 MHz, $CDCl_3$) δ 172.33, 142.72, 128.51, 127.75, 125.72, 70.33, 60.85, 43.49, 14.14.

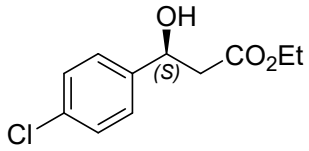

2b

Chiral HPLC method is show in Table S4. $[\alpha]_D^{25}$ = -40° (*c* 0.25, Chloroform). ^{1}H NMR (600 MHz, $CDCl_3$) δ 7.26-7.23 (m, 4H), 5.03 (dd, J_1=4.2 Hz, J_2= 9.0 Hz, 1H), 4.09 (q, *J* = 6.6 Hz, 2H), 3.85 (s, 1H), 2.61-2.57 (m, 2H), 1.18 (t, *J* = 7.2 Hz, 3H). ^{13}C NMR (151 MHz, $CDCl_3$) δ 171.9, 141.1, 133.3, 128.5, 127.1, 69.6, 60.9, 43.4, 20.9, 14.1.

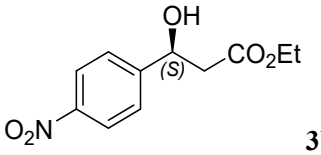

3b

Chiral HPLC method is show in Table S4. $[\alpha]_D^{28}$ = -38.2° (*c* 1.00, Chloroform). ^{1}H NMR (600 MHz, $CDCl_3$) δ 8.17 – 8.13 (m, 2H), 7.54 (d, *J* = 8.5 Hz, 2H), 5.21 (dd, *J* = 7.8, 4.8 Hz, 1H), 4.15 (q, *J* = 7.1 Hz, 2H), 3.91 (s, 1H), 2.71 (dd, *J* = 6.4, 3.2 Hz, 2H), 1.23 (t, *J* = 7.2 Hz, 3H). ^{13}C NMR (151 MHz, $CDCl_3$) δ 171.85, 150.00, 147.32, 126.55, 123.69, 69.36, 61.18, 43.07, 14.07.

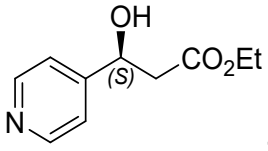

4b

Chiral HPLC method is show in Table S4. $[\alpha]_D^{25}$ = -30.3° (*c* 1.00, MeOH). ^{1}H NMR (400 MHz, DMSO-d_6) *δ* 8.55 – 8.49 (m, 2H), 7.42 – 7.36 (m, 2H), 5.80 (d, *J* = 5.0 Hz, 1H), 5.00 (dt, *J* = 9.1, 4.6 Hz, 1H), 2.76 – 2.54 (m, 2H), 1.17 (t, *J* = 7.1 Hz, 3H). ^{13}C NMR (101 MHz, DMSO-d_6) *δ* 170.28, 153.23, 149.40, 120.96, 68.18, 59.93, 43.50, 14.02.

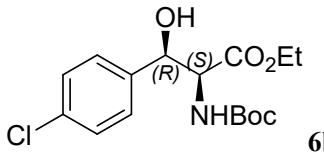

6b

Chiral HPLC method is show in Table S4. ^{1}H NMR (600 MHz, $CDCl_3$) δ 7.30 (s,4H), 5.40(d, *J* = 9.0 Hz, 1H), 5.18(s,1H), 4.63 (d, *J*=7.2 Hz, 1H), 4.19 (q, *J* = 6.3 Hz, 2H), 3.55 (s, 1H), 1.33 (s, 9H), 1.25 (t, 6.6Hz, 3H). ^{13}C NMR (151 MHz, $CDCl_3$) δ

170.8, 155.7, 138.6, 133.6, 128.4, 127.5, 80.2, 73.3, 61.8, 59.5, 28.1, 14.1.

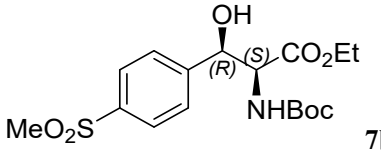

7b

Chiral HPLC method is show in Table S4. ^{1}H NMR (600 MHz, $CDCl_3$) δ 7.39 (d, *J* = 8.4 Hz, 2H), 7.50 (d, *J* =8.4 Hz, 2H), 5.44 (d, *J* = 9.6 Hz, 1H), 5.29 (s, 1H), 4.43 (d, *J* = 7.8 Hz, 1H), 4.29 (s, 1H), 4.15 (q, *J* = 7.2 Hz, 2H), 2.92 (s, 1H), 1.19 (s, 1H), 1.16 (t, 7.2 Hz, 3H). ^{13}C NMR (151 MHz, $CDCl_3$) δ 171.2, 155.6, 147.1, 139.3, 127.1, 127.0, 79.8, 72.8, 61.8, 60.3, 44.3, 28.0, 14.1.

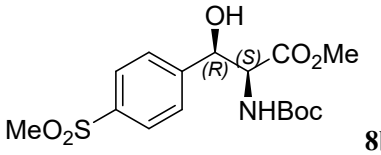

8b

Chiral HPLC method is show in Table S4. ^{1}H NMR (600 MHz, $CDCl_3$): *δ* = 7.85 (d, *J* = 8.16 Hz, 2 H), 7.57 (d, *J* = 8.28 Hz, 2 H), 5.37(s, 1 H), 5.34 (d, *J* = 9.06 Hz, 1 H), 4.55 (d, *J* = 8.52 Hz, 1 H), 3.80 (s,3 H), 3.27 (s, 1 H), 3.00 (s, 3 H), 1.29 (s, 9 H) ppm. ^{13}C NMR (150 MHz, $CDCl_3$): *δ* = 170.75, 155.53, 146.39, 139.74, 127.28, 127.16, 80.33,73.19, 59.09, 52.83, 44.49, 28.08 ppm. HRMS: calcd. for $C_{16}H_{27}N_2O_7S$ [M + NH_4]$^{+}$ 391.1533; found 391.1532.

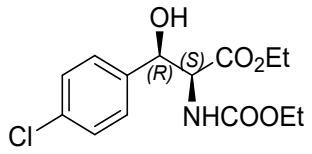

9b

Chiral HPLC method is show in Table S4. ^{1}H NMR (600 MHz, $CDCl_3$) δ 7.30-7.27 (m, 4H), 5.66 (d, *J* = 9.0 Hz, 1H), 5.17 (s, 1H), 4.95 (d, *J* = 6.6 Hz, 2H), 4.17 (q, *J* = 6.6 Hz, 2H), 3.96(q, *J* = 6.6 Hz, 2H), 1.24 (t, *J* = 7.2 Hz, 3H), 1.14 (t, *J* = 7.2 Hz, 3H). ^{13}C NMR (151 MHz, $CDCl_3$) δ170.1, 155.7, 138.5, 133.7, 128.4, 127.5, 73.0, 61.9, 61.4, 59.8, 14.4, 14.1.

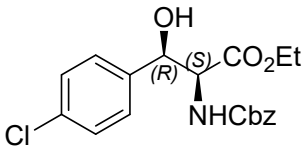

10b

Chiral HPLC method is show in Table S4. ^{1}H NMR (600 MHz, $CDCl_3$) δ 7.35-7.22 (m, 9H), 5.77 (d, *J* = 9.0 Hz, 1H), 5.24 (s, 1H), 4.98 (q, *J* = 12.6 Hz, 2H), 4.75 (d, *J* = 9.0 Hz,1H), 4.21-4.19 (m, 2H), 3.5 (s, 1H), 1.26 (t, *J* = 6.6 Hz, 3H). ^{13}C NMR (151 MHz, $CDCl_3$) δ 170.6, 156.4, 138.3, 136.1, 133.7, 128.5, 128.2, 127.9, 127.4, 73.0, 67.1, 62.0, 59.8, 14.1.

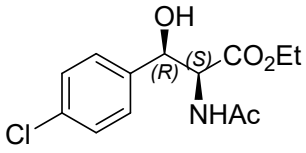

11b

Chiral HPLC method is show in Table S4. ^{1}H NMR (600 MHz, $CDCl_3$) δ8.18 (d, J=9.0 Hz, 2H), 7.40 (d, *J* = 8.4 Hz, 2H), 7.36 (d, *J* = 8.4 Hz, 2H), 5.95 (d, *J* = 4.8 Hz,

1H), 5.10 (t, J = 4.2 Hz, 1H), 4.56 (dd, J_1=3.6Hz, J_2= 8.4 Hz, 1H), 4.10-4.06 (m, 1H), 1.79 (s, 3H), 1.15 (t, J = 7.2 Hz, 3H). ^{13}C NMR (151 MHz, $CDCl_3$) δ 170.6, 170.1, 141.3, 132.2, 128.7, 128.1, 72.2, 61.0, 58.7, 22.6, 14.4.

2. Supporting Schemes, Tables and Figures

Scheme S1. Synthesis of Chloramphenicol via WTEA biocatalysis.

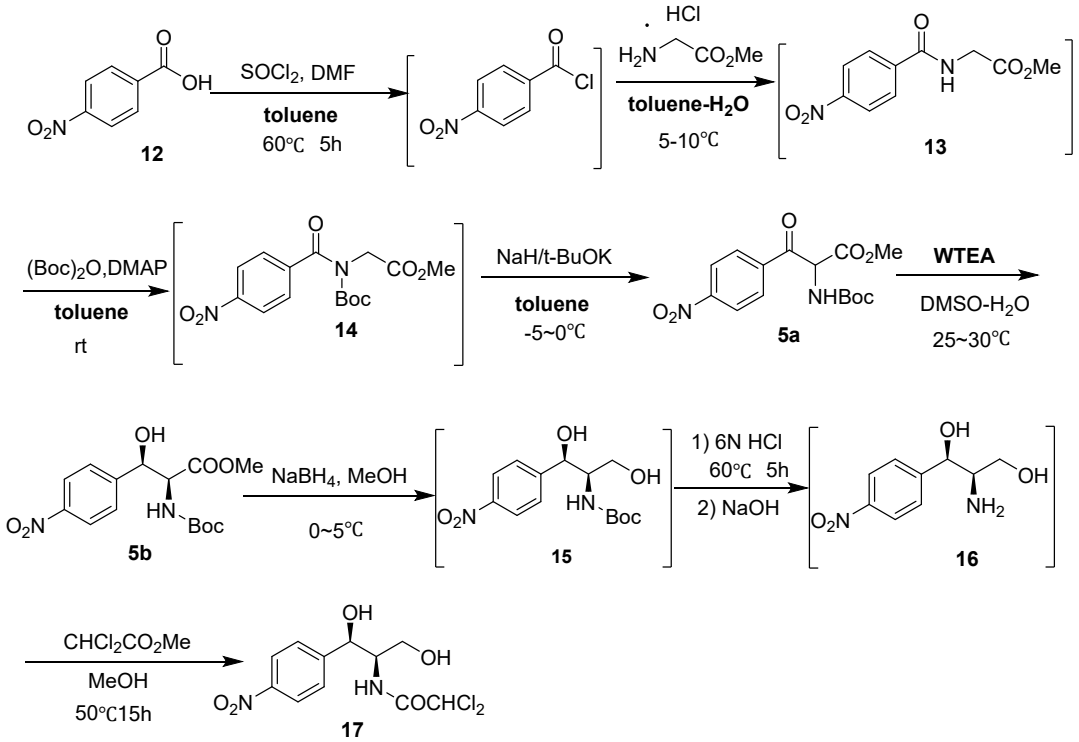

Scheme S2. Synthesis of Chloramphenicol via Mutant M30 biocatalysis.

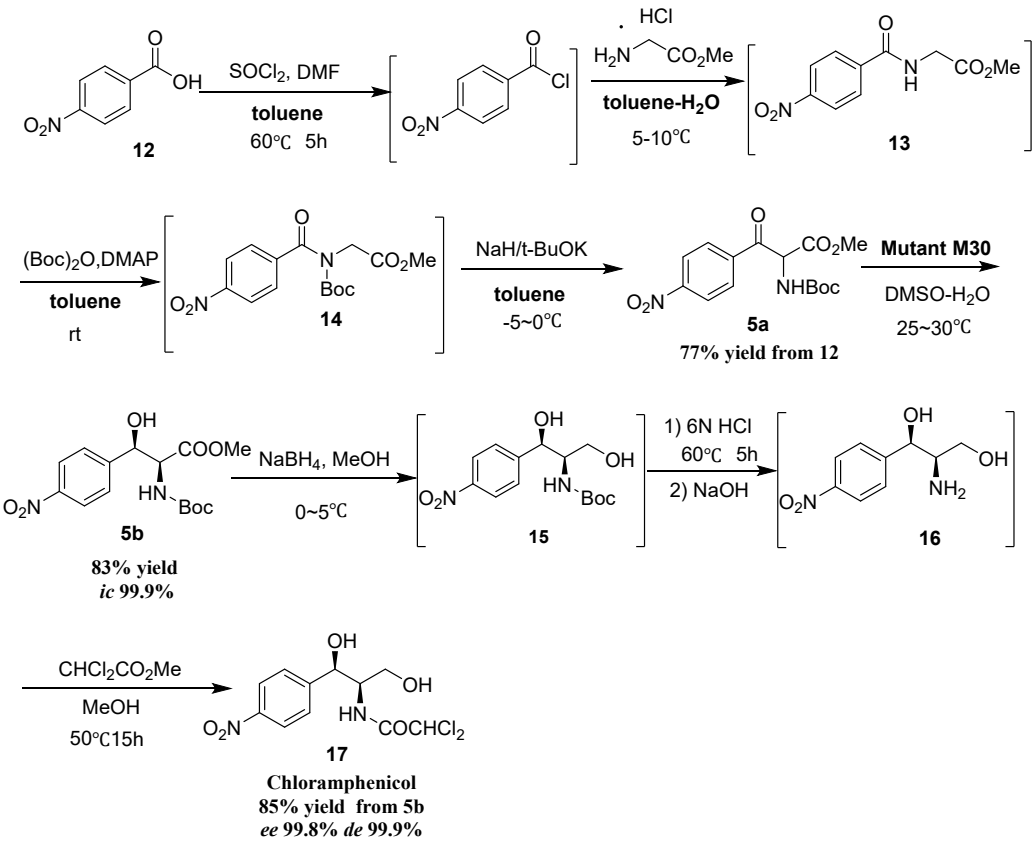

Table S1. Crystallographic Data Collection and Refinement Statistics

	WTEA	M20	M30
Data collection			
Space group	C2221	P21221	P1211
Cell dimensions			
a, b, c (Å)	86.98, 134.94, 81.41	68.46, 71.16, 115.16	71.33, 68.66, 114.68
α, β, γ (degree)	90, 90, 90	90, 90, 90	90, 90, 90
Resolution (Å)	43.49-2.25 (2.29-2.25)	50.00-2.60 (2.64-2.60)	34.08-2.72 (2.79-2.72)
Completeness (%)	99.9 (99.4)	97.7 (95)	99.9 (95.9)
Mean *I*/sigma (*I*)	11.8 (2.8)	1.6 (1.4)	6.7 (1.9)
Rmerge	0.101 (0.469)	0.268 (0.992)	0.211 (0.598)
CC1/2	0.996 (0.883)	0.948 (0.570)	0.949 (0.712)
Redundancy	6.2 (5.5)	4.8 (3.9)	3.4 (3.5)

Refinement			
R_{work}/R_{free}	0.21/0.25	0.21/0.26	0.21/0.25
B-factors (Å^2)			
Protein	39.28	28.07	30.11
Ligand	110.72	28.67	28.41
Water	33.14	29.14	18.33
No. atom			
Protein	3496	3830	7638
Ligand/ion	48	96	192
Water	87	48	82
r.m.s.d. Bond lengths (Å)	0.0180	0.0145	0.0065
r.m.s.d. Bond angles (°)	1.985	1.749	1.495
Most favored (%)	96.17	95.33	95.24
Allowed (%)	2.83	3.86	4.15
Disallowed (%)	0.90	0.81	0.61
PDB entry	7E28	7E3X	7E24

Values in parentheses are for the outermost resolution shells.

Table S2. Sequences of Mutagenesis Primers Used for Construction of WTEA Variants.

Primmers	Template	Sequence (5' to 3')
WTEA F	WTEA	taagaaggagatatacatatgaaatacaccgttatcaccg
WTEA R		tggtgtgcggccgcaaagcttttaaccagcgtagttgaac
Y15R1		ggtttcYNBaccgataccagaagaagcaccggtgataacgg
Y15F2		ctggtatcggtVNRgaaaccgctaaactgcttgctggtaaa
V67 R1		tacaggtcgtgRVNgttctggttgtcagccaggtcaacaga
V67 F2		cagaacNBYcacgacctgtacgaaggtctgaaagaactgga
F88 R1		tcgaagtcaccRMYaccagcgttgttgatccaggtttcgat
F88 F2		gctggtRKYggtgacttcgacctggttcaggacatcgaact
K101R1		ttcgatBYSacccagttcgatgtcctgaaccaggtcgaagt
K101F2		tcgaactgggtSRVatcgaaaaaatgctgcgtctgaacatc
K104R1		cagcatBBBttcgattttacccagttcgatgtcctgaacca
K104F2		gtaaaatcgaaVVVatgctgcgtctgaacatcgaagctctg
A138 R1		cggtaaccaccTRHagaagagatgttaaccagggtggtacc
A138 F2		tcttctDYAggtggttaccgtatcgttccgaacgctgttac
R142 R1		aacgatSWDgtaaccacccgcagaagagatgttaaccaggg

R142 F2		gggtggttacHWSatcgttccgaacgctgttacctactgc
V144 R1		gttcggRMSgatacggtaaccacccgcagaagagatgttaa
V144 F2		gttaccgtatcSKYccgaacgctgttacctactgcgctacc
A183G R1		ggtagcAcccggagccagaactttagcacgcagtttagcac
A183G F2		ttctggctccgGGTgctaccgaaaccgaattcgctgaccgt
A190 R1		cggctacggtcRDHgaattcggtttcggtagcagccggagc
A190 F2		gaattcDHYgaccgtagccgtggtgaagctggtttcgacta
R192 R1		acggctDYBgtcagcgaattcggtttcggtagcagccggag
R192 F2		aattcgctgacVRHagccgtggtgaagctggtttcgactac
S193 R1		accacgRSGacggtcagcgaattcggtttcggtagcagccg
S193 F2		tcgctgaccgtGSYcgtggtgaagctggtttcgactactct
Y201 R1		tttagaMNNgtcgaaaccagcttcaccacggctacggtca
Y201 F2		ctggtttcgacNNKtctaaaaacgttaaaaaataccacacc
L28V R1		cagaacaacagatttacctttaccagccagcagtttagcgg
L28V F2		aaggtaaatctgttgttctggttgctcgtcgtacctctgaa
E80D R1		ccaggtgtcgatgtccagttctttcagaccttcgtacaggt
E80D F2		aactggacatcgacacctggatcaacaacgctggtttcggt
W82L R1		gttgatcagggtttcgatgtccagttctttcagaccttcgt
W82L F2		acatcgaaaccctgatcaacaacgctggtttcggtgacttc
H124M R1		gtcgtgcatgtcacgaacgaacagagaagacaggatggtca
H124M F2		tcgttcgtgacatgcacgacatcgaaggtaccaccctggtt
L132I R1		gttaacgatggtggtaccttcgatgtcgtggtggtcacgaa
L132I F2		aaggtaccaccatcgttaacatctcttctgcgggtggttac
L175I R1		agcacggattttagcaccacctttctgcagttcctgagcca
L175I F2		gtggtgctaaaatccgtgctaaagttctggctccggctgct
A177V R1		aactttaacacgcagtttagcaccacctttctgcagttcct
A177V F2		ctaaactgcgtgttaaagttctggctccggctgctaccgaa
AS190-193VA R1		cgagcacggtcaacgaattcggtttcggtagcagccggagc
AS190-193VA F2		gaattcgttgaccgtgctcgtggtgaagctggtttcgacta
V67LP R1	M1	tacaggtcgtgRRGgttctggttgtcagccaggtcaacaga
V67LP F2		cagaacCYYcacgacctgtacgaaggtctgaaagaactgga
F88 R1		tcgaagtcaccRMYaccagcgttgttgatccaggtttcgat
F88 F2		gctggtRKYggtgacttcgacctggttcaggacatcgaact
AR138-142 R1		aacgatSWDgtaaccaccTRHagaagagatgttaaccaggg
AR138-142 F2		ggtggttacHWSatcgttccgaacgctgttacctactgc
W82L R1	M20	gttgatcagggtttcgatgtccagttctttcagaccttcgt
W82L F2		acatcgaaaccctgatcaacaacgctggtgttggtgacttc
LL175-168 R1		agcacgARYtttagcaccacctttctgARCttcctgagcca
LL175-168 F2		gtggtgctaaaRYTcgtgctaaagttctggctccggctgct
V121A R1		tggtggtcacgagcgaacagagaagacaggatggtcagagc
V121A F2		ctgttcgctcgtgaccaccacgacatcgaaggtaccaccct
N204AG R1		tatttttttaacASCtttagagtagtcgaaaccagcttcacc
N204AG F2		tctaaaGSTgttaaaaaataccacaccgctgctgaaatggc
Y201F R1		tttagagaagtcgaaaccagcttcaccacgagcacggtca

Y201F F2	ctggtttcgacttctctaaaaacgttaaaaaataccacacc

M:(A/C); V:(A/C/G); R:(A/G); H:(A/C/T); W:(A/T); D:(A/G/T); S:(C/G); B:(C/G/T); Y:(C/T); N:(A/G/C/T); K:(G/T)

M1: A190V/S193A; M20: F88V/A138L/R142M/A190V/S193A

Table S3. WTEA Variants

	Mutated residues
M1	A190V、S193A
M2	R142F、A190V、S193A
M3	R142M、A190V、S193A
M4	A138V、R142F、A190V、S193A
M5	R142L、A190V、S193A
M6	A138V、R142L、A190V、S193A
M7	A138L、R142L、A190V、S193A
M8	F88V、R142M、A190V、S193A
M9	F88I、R142L、A190V、S193A
M10	F88I、R142M、A190V、S193A
M11	F88I、R142F、A190V、S193A
M12	F88V、R142L、A190V、S193A
M13	F88S、R142H、A190V、S193A
M14	F88V、A138V、R142L、A190V、S193A
M15	F88I、A138L、R142I、A190V、S193A
M16	F88I、A138L、R142F、A190V、S193A
M17	F88I、A138L、R142L、A190V、S193A
M18	F88V、A138L、R142L、A190V、S193A
M19	F88I、A138L、R142M、A190V、S193A
M20	F88V、A138L、R142M、A190V、S193A

Table S4. HPLC Conditions and Retention Times for Target Compounds [a].

Compounds	Column	Mobile phase	Detection (nm)	Retention time (min)
1b	IC-3[b]	hexane: ethanol=95:5	210	11.4 min (*R*), **11.9 min (*S*)**
2b	IC-3	hexane: ethanol=95:5	210	8.8 min (*R*), **9.3 min (*S*)**
3b	IC-3	hexane: ethanol=95:5	210	20.6 min (*R*), **21.5 min (*S*)**
4b	IC-3	hexane: ethanol=95:5	254	**11.9 min (*S*),** 14.3 min (*R*)
5b	IB-3[c]	hexane: isopropanol=95:5	254	22.0 min, 26.8 min, **38.7 min,** 46.8 min
6b	OJ-H[d]	hexane: isopropanol=95:5	210	8.3 min, **10.3 min,** 11.6 min, 15.8 min
7b	IB-3	hexane: ethanol=95:5,	220	32.2 min, 34.3 min,

		(0.1% Diethylamine, 0.1% trifluoroacetic acid)		**37.9 min,** 39.1 min
8b	IB-3	hexane: ethanol=95:5, (0.1% Diethylamine,0.1% trifluoroacetic acid)	220	38.7 min, 41.1 min, **44.9 min,** 59.9 min
9b	OJ-H	hexane: isopropanol =93:7	210	12.3 min, **14.7 min,** 17.3 min, 30.9 min
10b	OJ-H	hexane: isopropanol =32:68	210	**5.4 min,** 5.7 min, 6.3 min, 7.2 min
11b	OJ-H	hexane: isopropanol =93:7	210	16.1 min, 19.4 min, **21.9 min,** 23.6 min

[a]General HPLC condition: temperature: 30 °C; flow rate: 1 mL/min

[b]IC-3: CHIRALPAK IC-3 column (3 μm, 4.6 mm× 250 mm, DAICEL, Shanghai)

[c]IB-3: CHIRALPAK IB-3 column (3 μm, 4.6 mm× 250 mm, DAICEL, Shanghai)

[d]OJ-H: CHIRALPAK IB-3 column (5 μm, 4.6 mm× 250 mm, DAICEL, Shanghai)

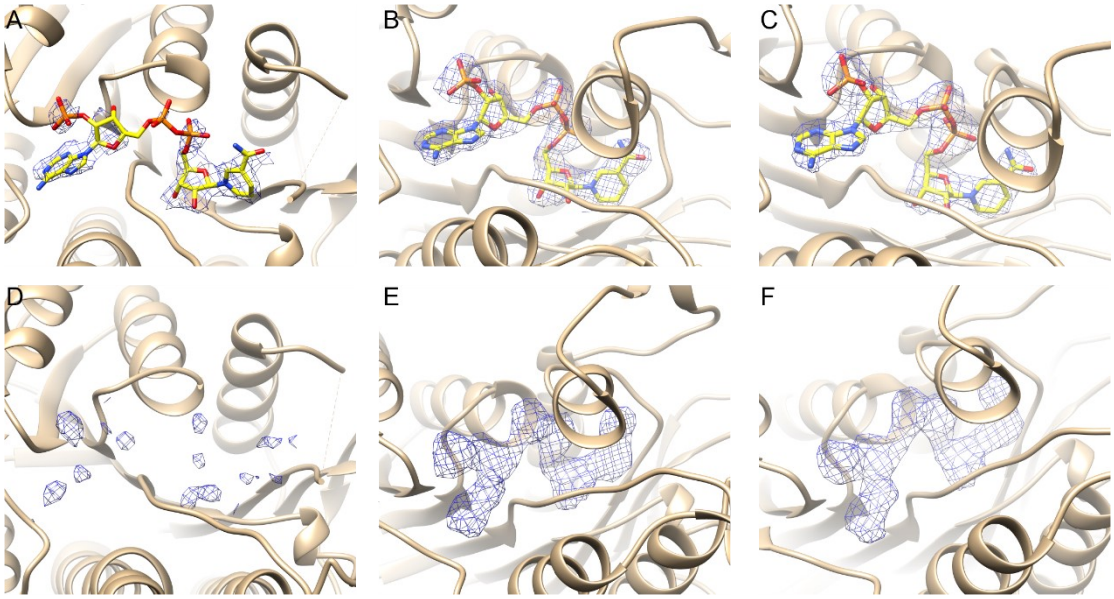

Figure S1. Electron density in the $NADP^+$ binding site. Final 2Fo-Fc electron density map (blue mesh), in WTEA (A), M20 (B), and M30 (C) $NADP^+$ binding site, contoured at 1.3 RMSD. The 2Fo-Fc omit density map (blue mesh) is contoured at 1.3 RMSD for WTEA (D), M20 (E), and M30 (F).

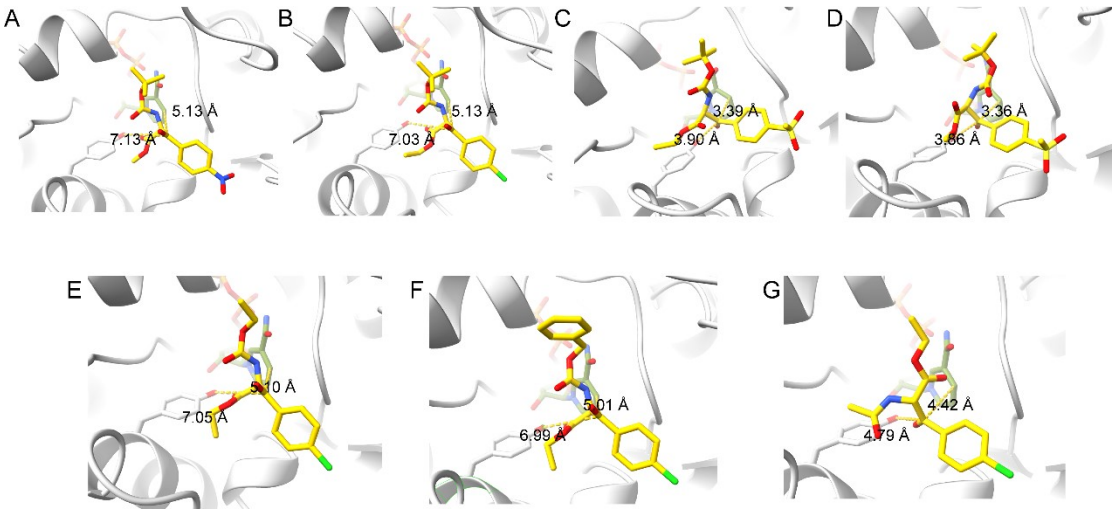

Figure S2. Molecular dock analysis of substrates **5a-11a** (A-G) into the binding pocket of WTEA. Dashed lines dictate distances between ketone carbon of substrate with oxygen atom of Y150 side chain and C_4 atom of cofactor $NADP^+$, respectively. The best substrate bind orientation (judged by the distance of Y150-substrate and NADPH-substrate) was selected in each run.

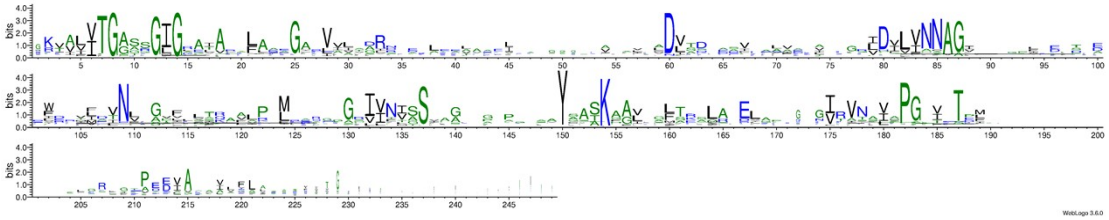

Figure S3. Deep Multiple Sequence Alignment (DeepMSA) of WTEA

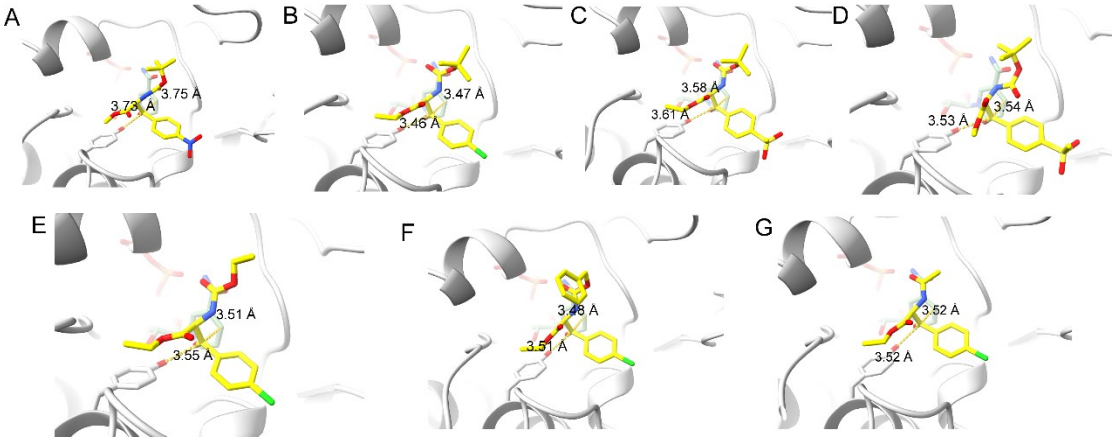

Figure S4. Molecular dock analysis of substrates **5a-11a** (A-G) into the binding pocket of M20. Dashed lines dictate distances between ketone carbon of substrate with oxygen atom of Y150 side chain and C4 atom of cofactor $NADP^+$, respectively. The best substrate bind orientation (judged by the distance of Y150-substrate and NADPH-substrate) was selected in each run.

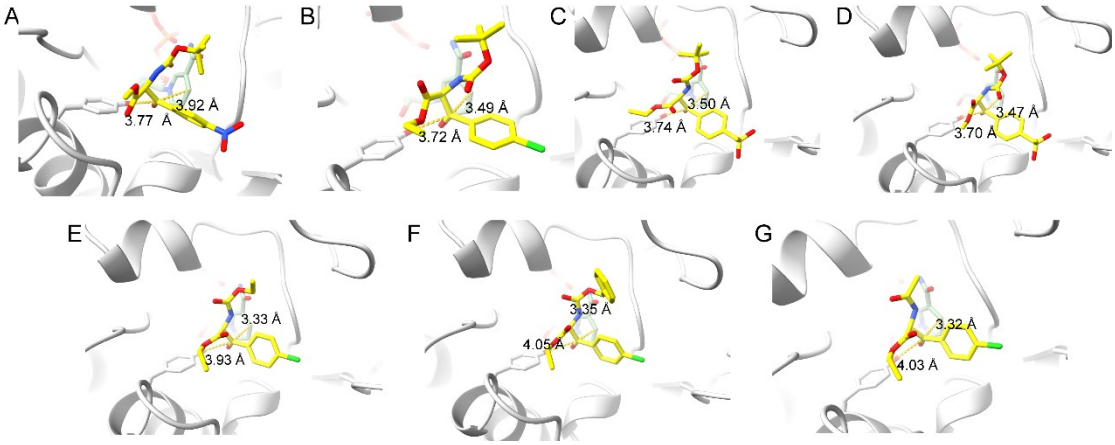

Figure S5. Molecular dock analysis of substrates **5a-11a** (A-G) into the binding pocket of M30. Dashed lines dictate distances between ketone carbon of substrate with oxygen atom of Y150 side chain and C4 atom of cofactor $NADP^+$, respectively. The best substrate bind orientation (judged by the distance of Y150-substrate and NADPH-substrate) was selected in each run.

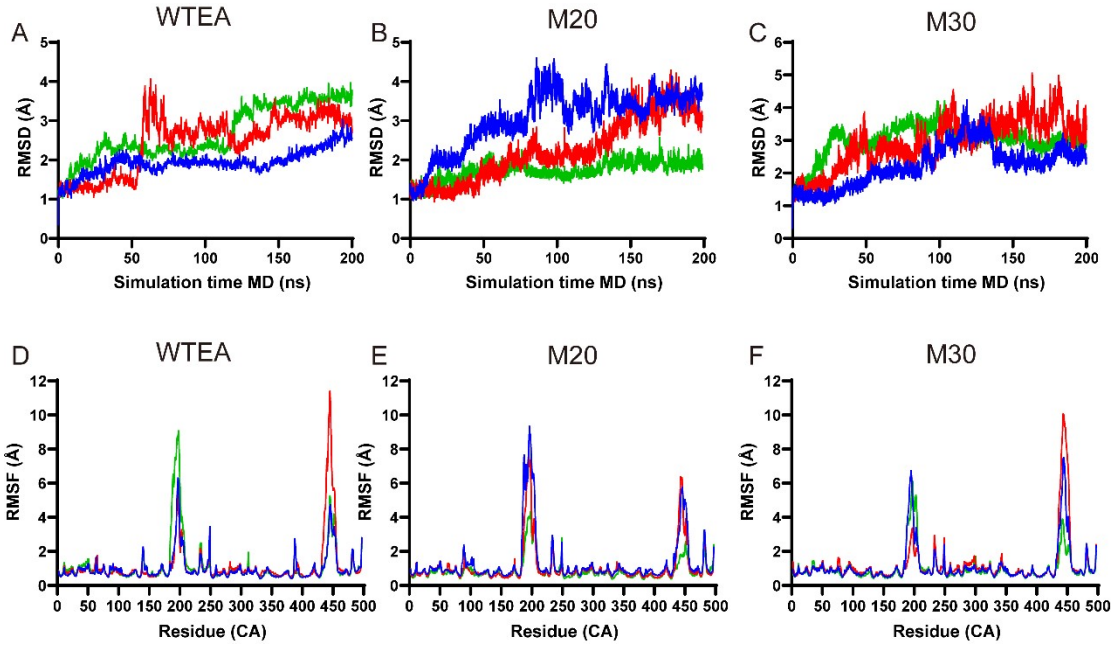

Figure S6. MD simulations analysis of the overall conformation of WTEA and mutants. RMSD analysis of WTEA (A), M20 (B), and M30 (C) was computed from 3 replicas of 200 ns of MD simulations. RMSF analysis of alpha carbons of WTEA (D), M20 (E), and M30 (F) was calculated from 3 replicas of 200 ns of MD simulations, residue 298-497 represent another protein chain.

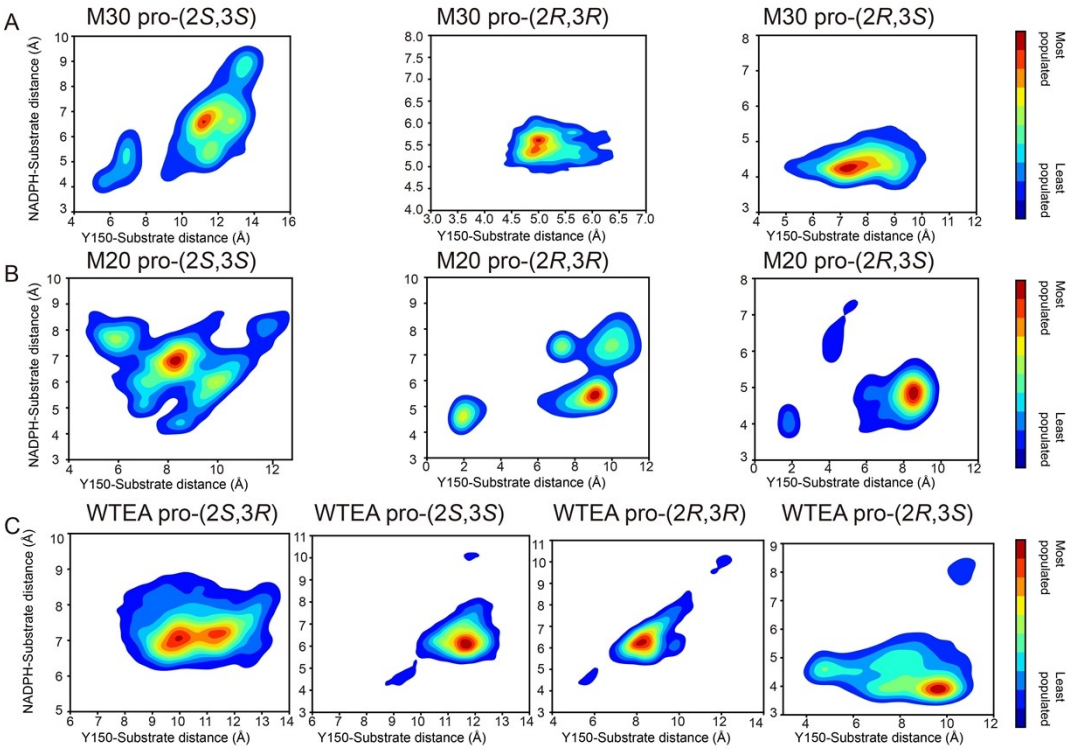

Figure S7. Analysis of prereaction states. Conformational distribution of (A) M30 and (B) M20 and (C) WTEA with docked substrate-**9a**. The conformation satisfying both Y150-Substrate distance ≤ 3.4 Å and NDPH-Substrate ≤ 4.5 Å was used for calculating the population of prereaction states. The starting conformations of pro-(2*S*, 3*R*), pro-(2*S*, 3*S*), pro-(2*R*, 3*R*) and pro-(2*R*, 3*S*) orientations were obtained from in silico dock.

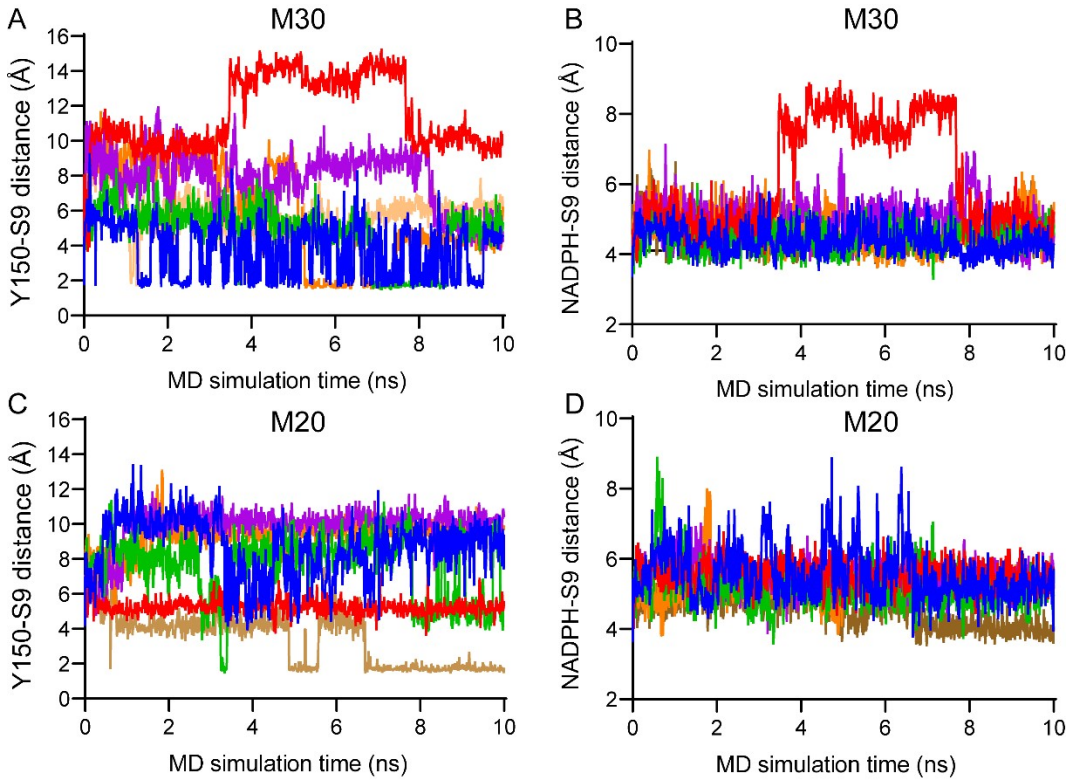

Figure S8. MD simulations analysis of the prereaction state of WTEA and mutants. (A) Plot of the distance between the residue Y150 of M30 and docked substrate **9a**. (B) Plot of the distance between the cofactor NADPH of M30 and docked substrate **9a**. (C) Plot of the distance between the residue Y150 of M20 and docked substrate **9a**. (D) Plot of the distance between the cofactor NADPH of M20 and docked substrate **9a**.

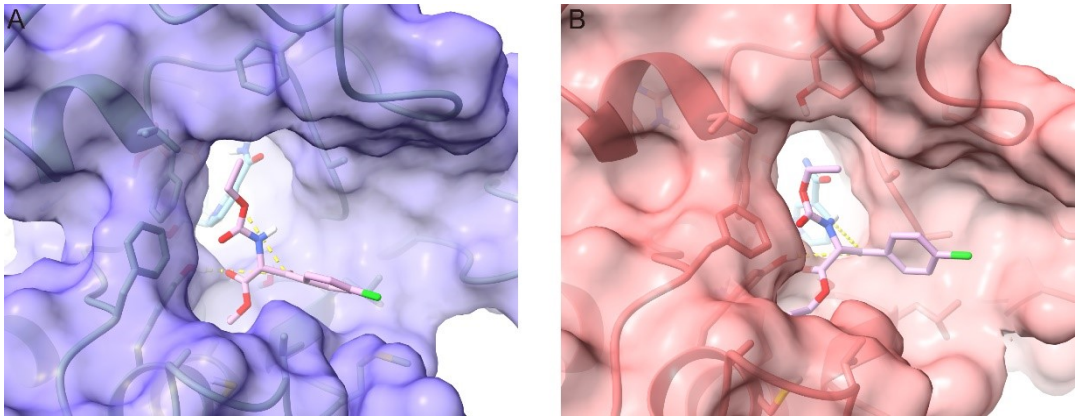

Figure S9. (A) Representative pro-(*2R*, *3R*) substrate **9a** orientation in M30. (B) Possible catalytic compatible representative pro-(*2R*, *3R*) substrate **9a** orientation in M20.

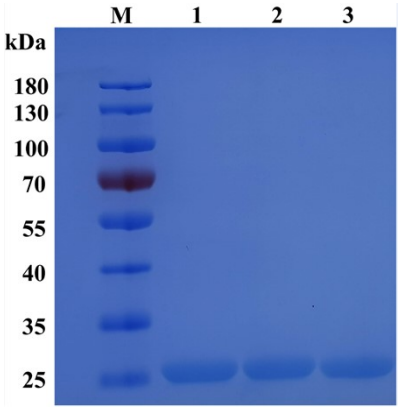

Figure S10. SDS-PAGE analysis of WTEA, mutant M20, and mutant M30. M: protein markers;1: WTEA; 2: mutant M20; 3: mutant M30

3. NMR spectra

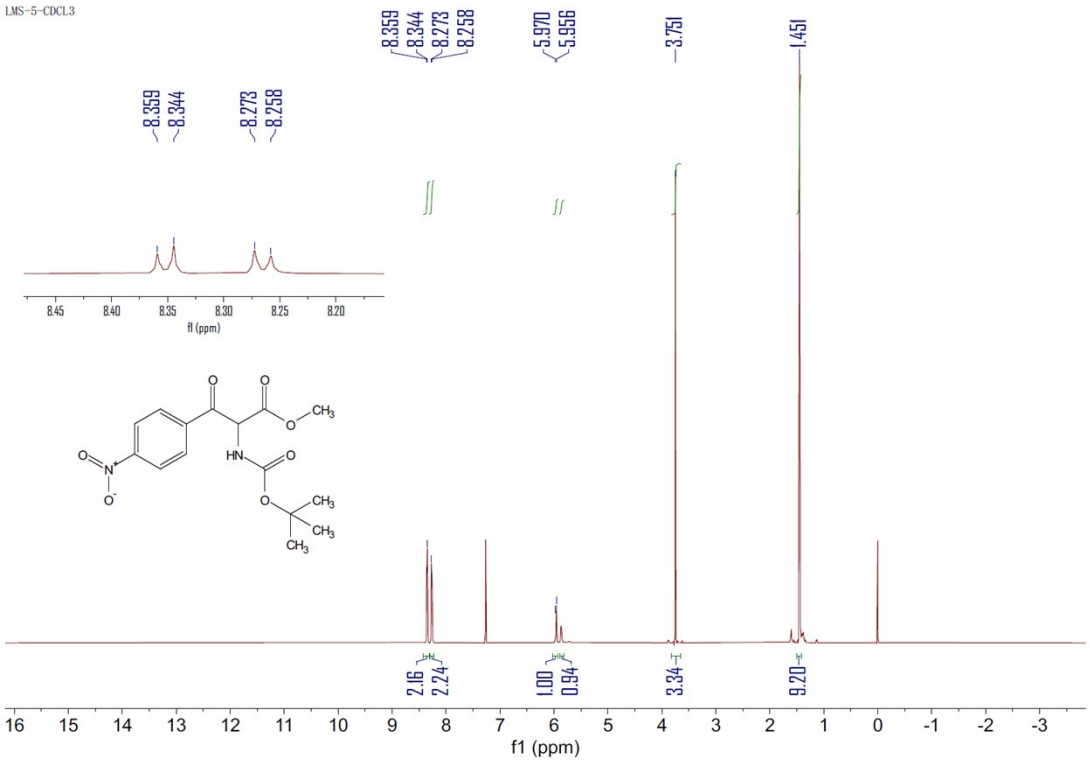

Figure S11. ^{1}H NMR spectrum of compound **5a**

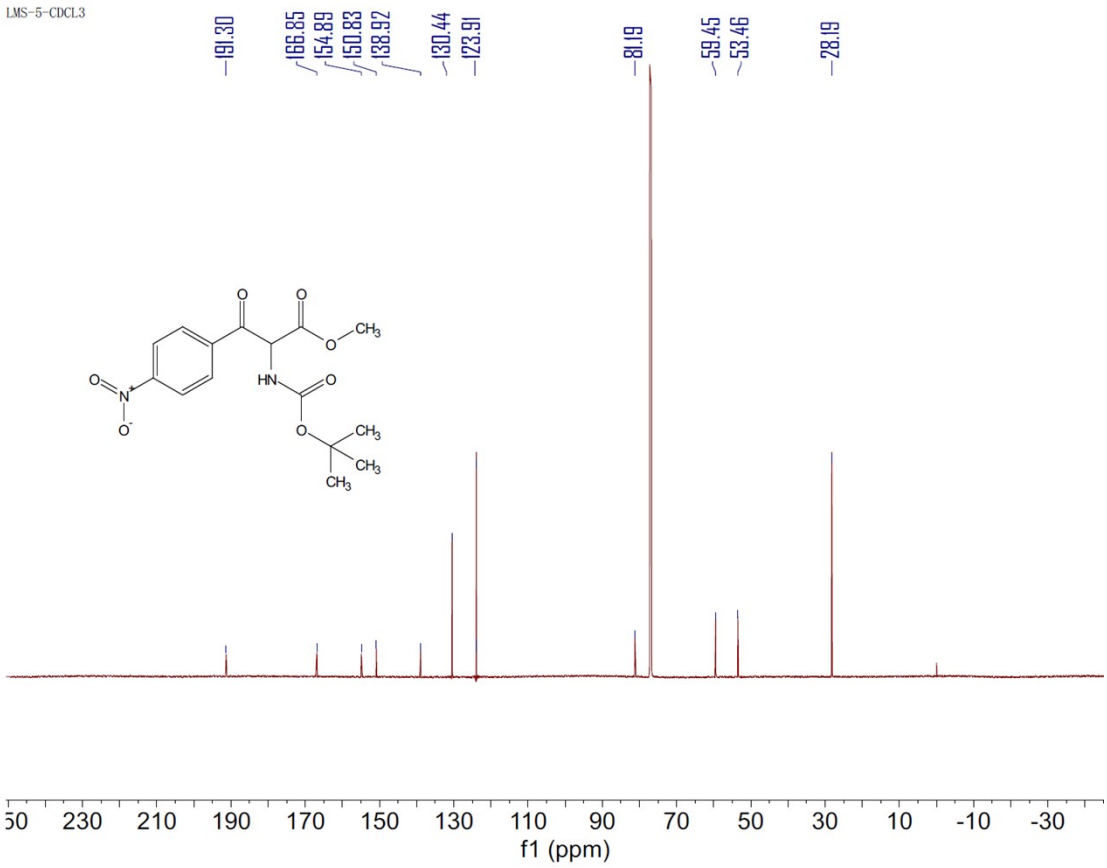

Figure S12. ^{13}C NMR spectrum of compound **5a**

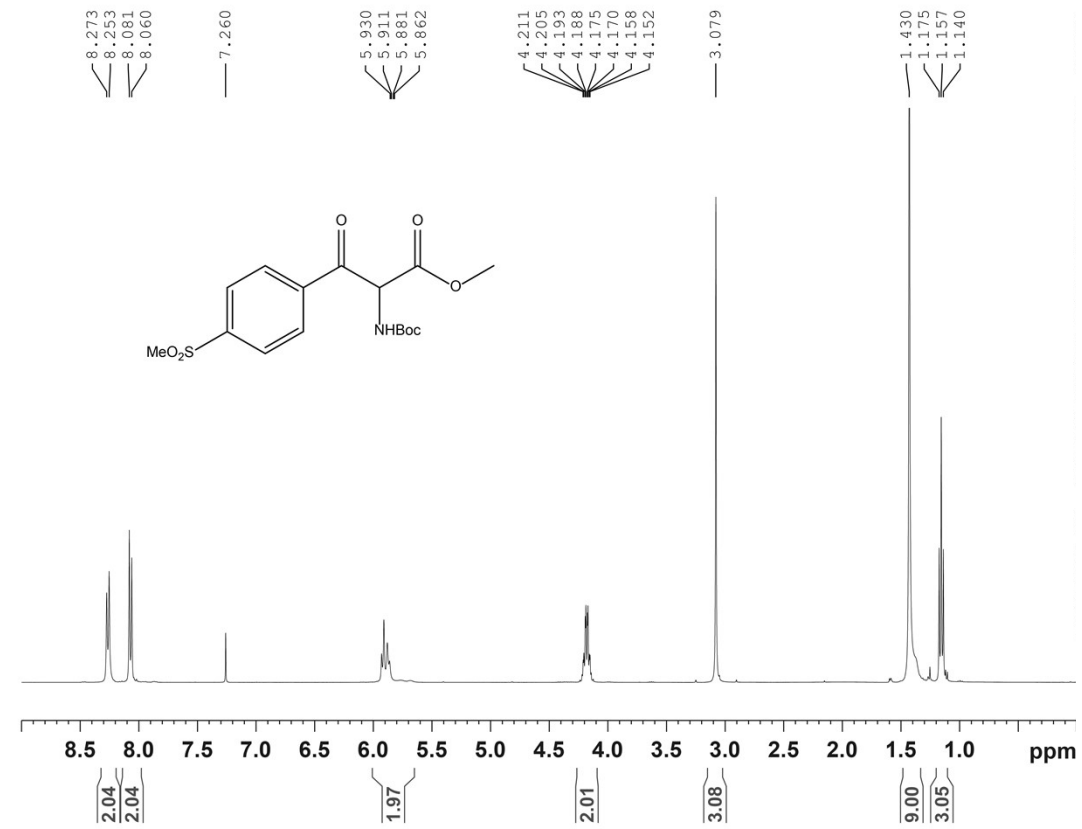

Figure S13. ^{1}H NMR spectrum of compound **7a**

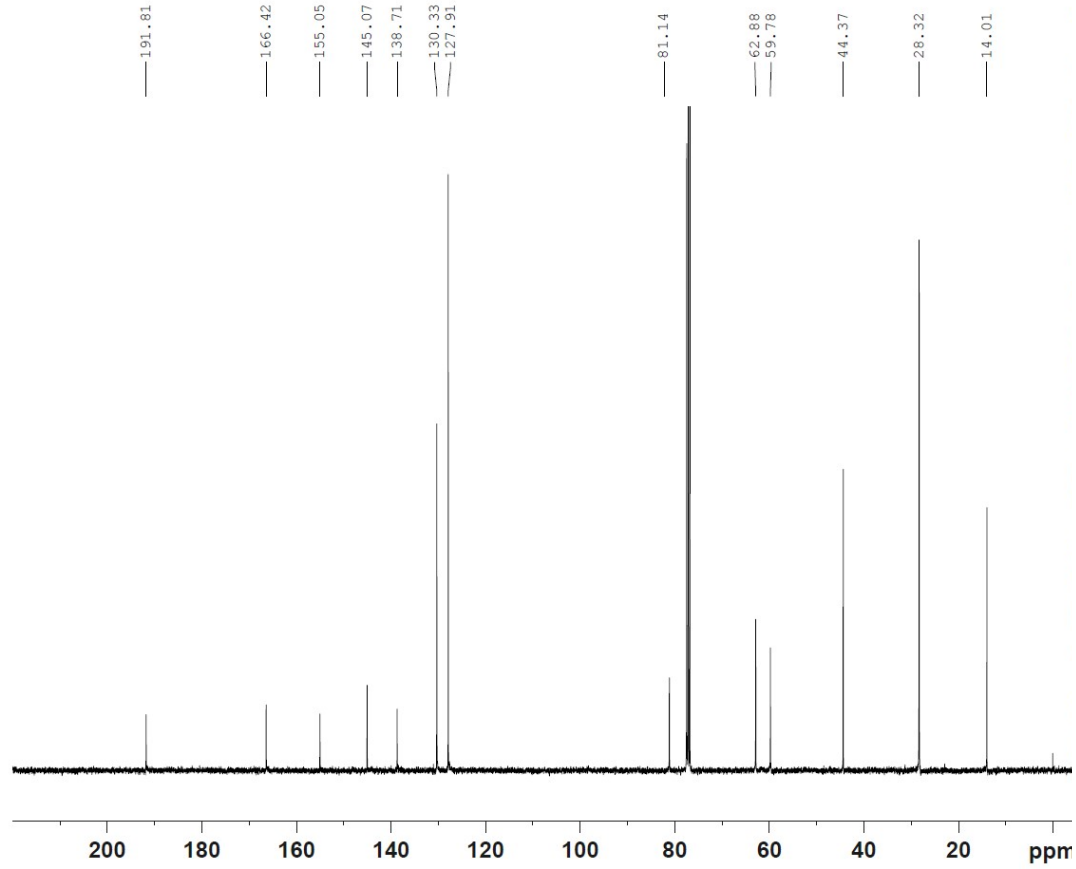

Figure S14. ^{13}C NMR spectrum of compound **7a**

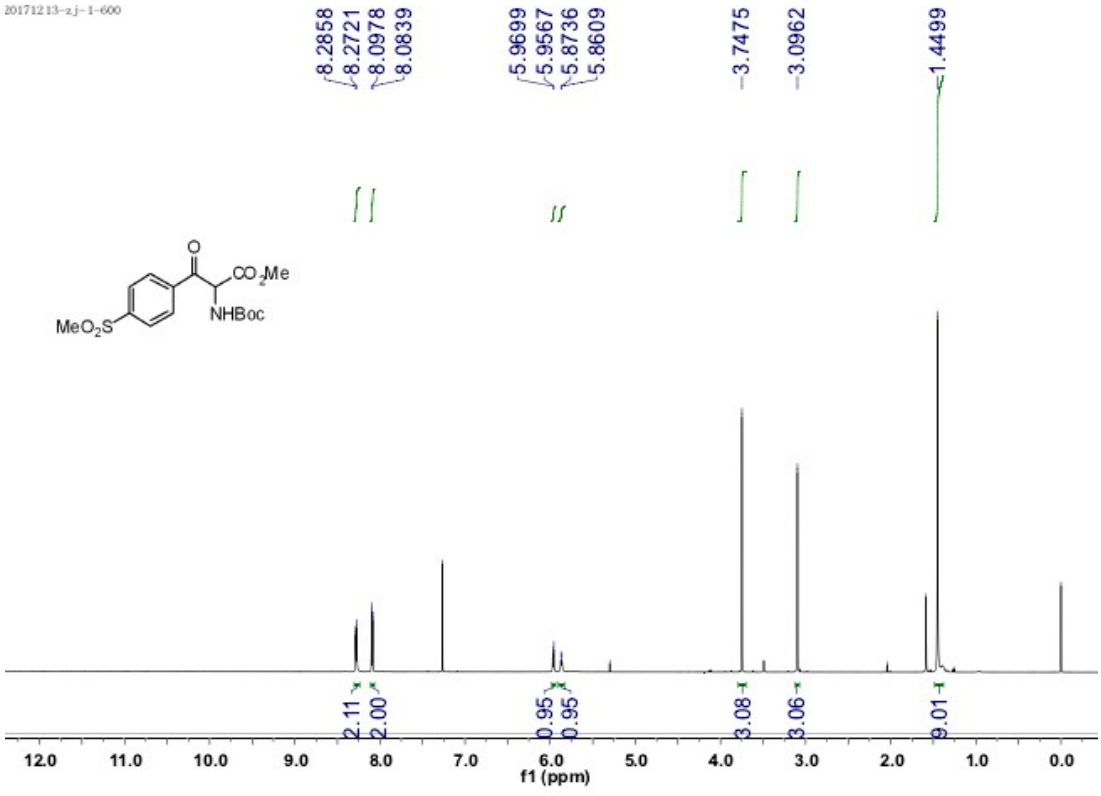

Figure S15. ^{1}H NMR spectrum of compound **8a**

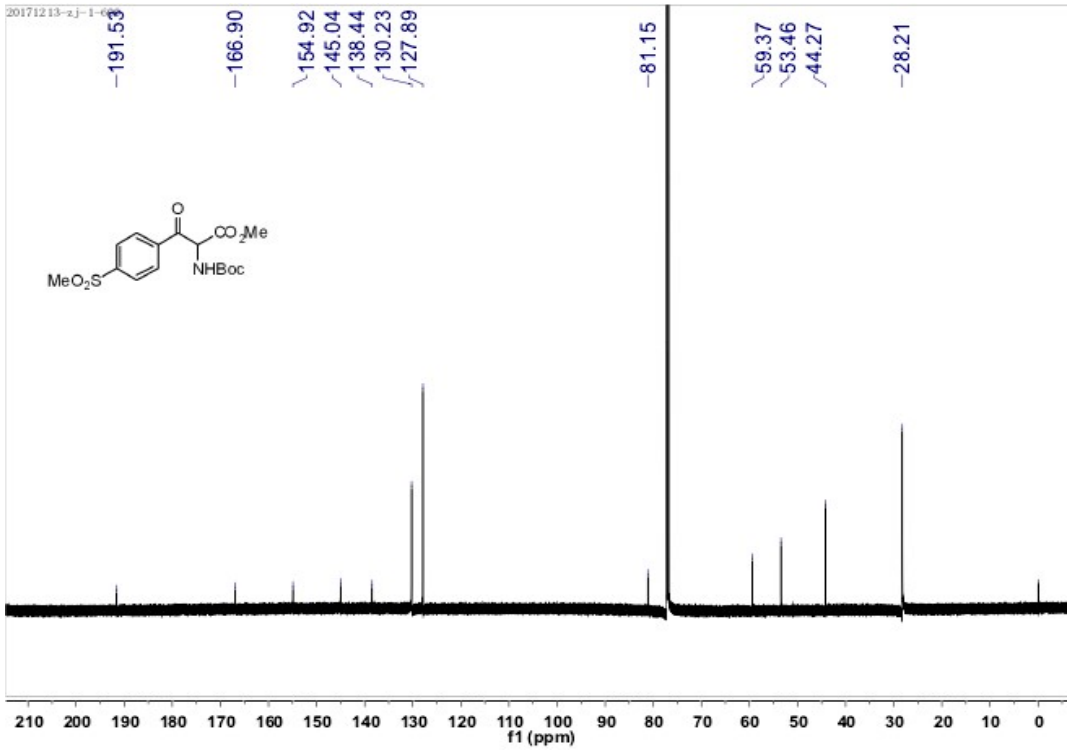

Figure S16. ^{13}C NMR spectrum of compound **8a**

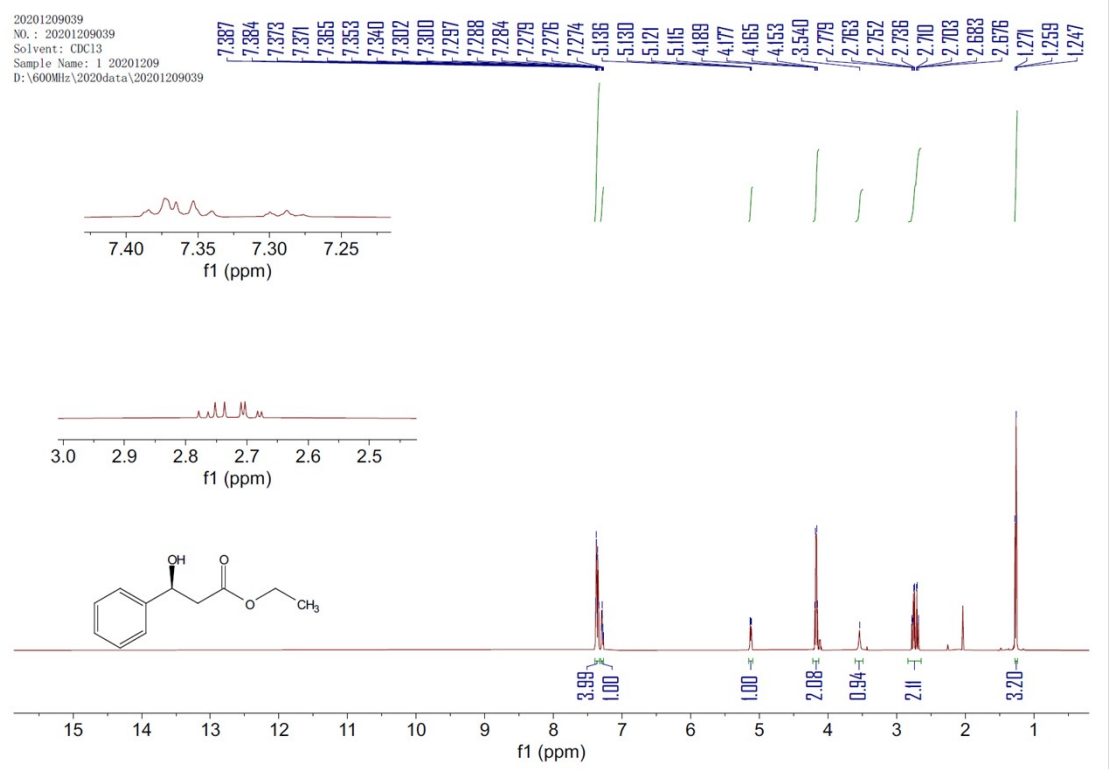

Figure S17. ^{1}H NMR spectrum of compound **1b**

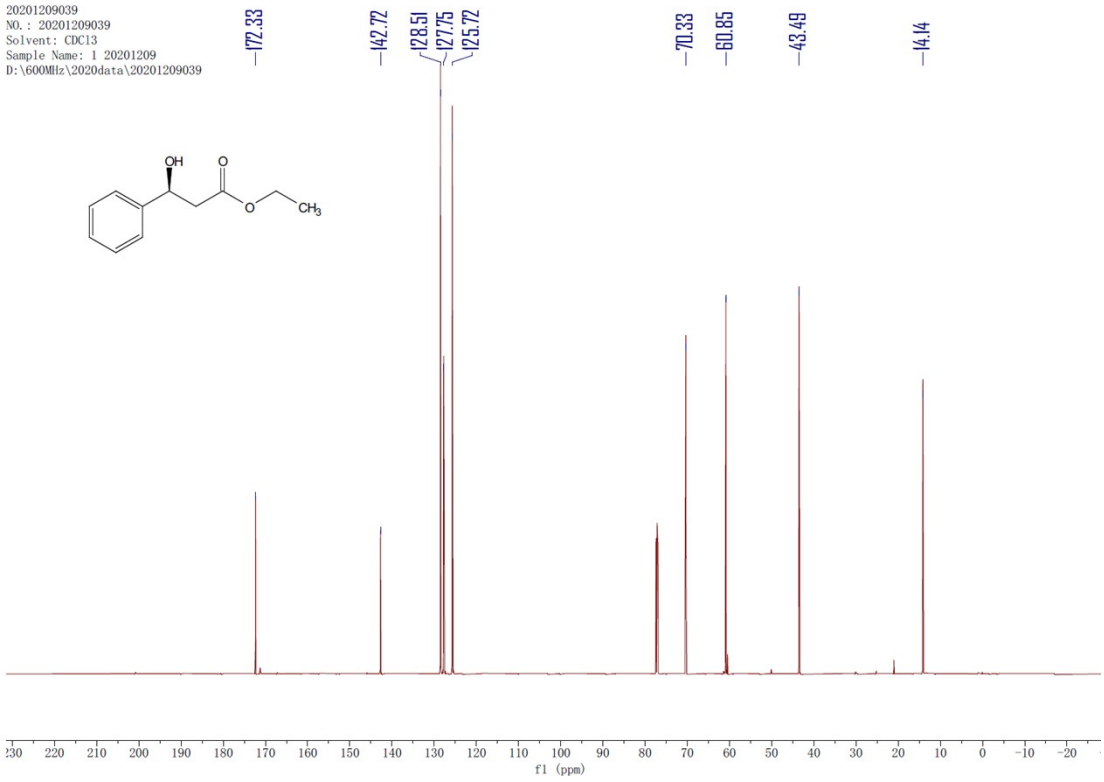

Figure S18. ^{13}C NMR spectrum of compound **1b**

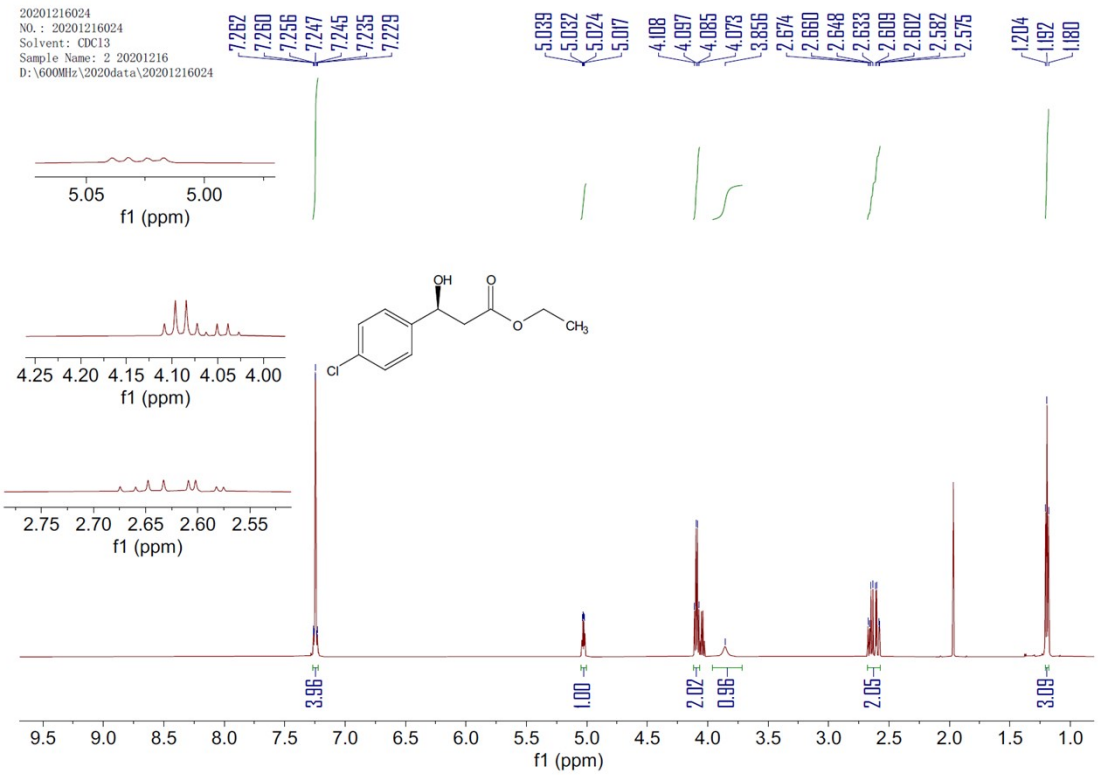

Figure S19. ^{1}H NMR spectrum of compound **2b**

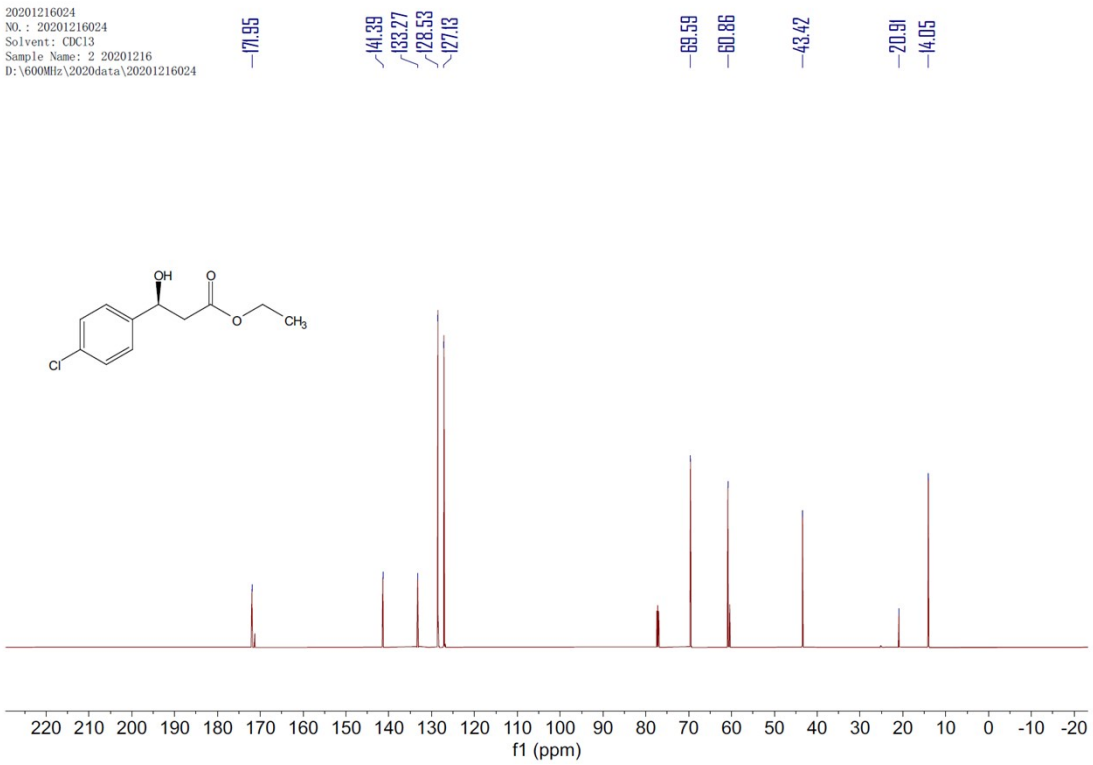

Figure S20. ^{13}C NMR spectrum of compound **2b**

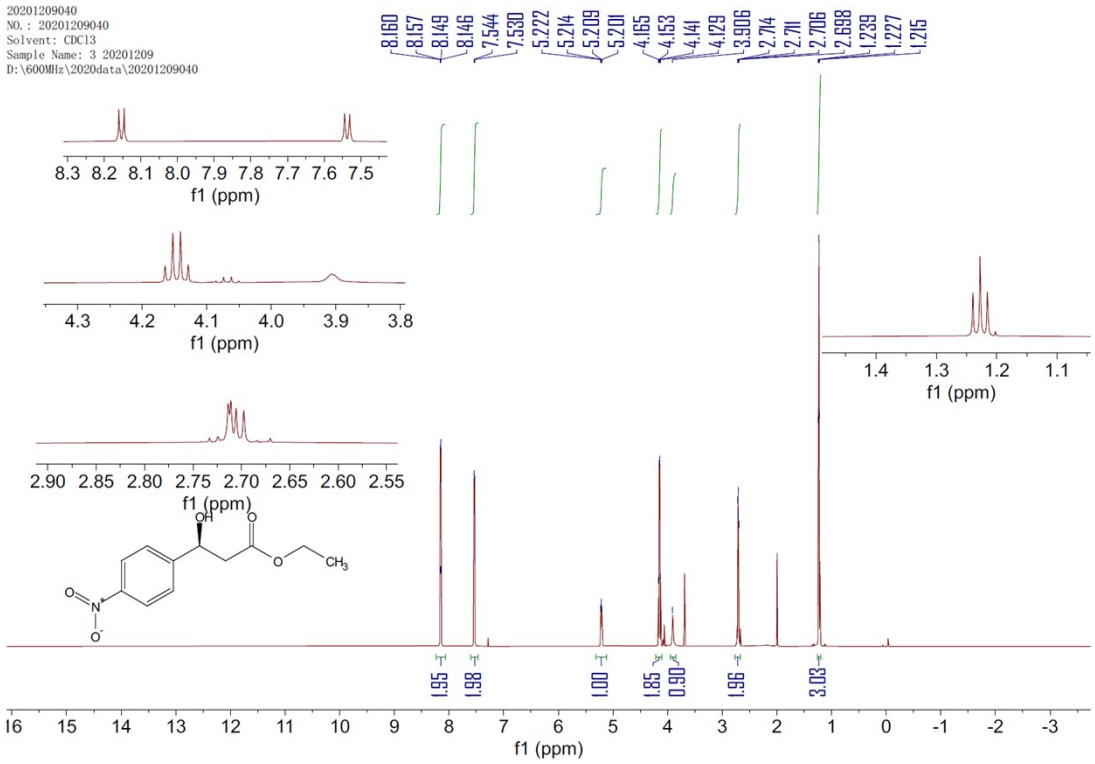

Figure S21. ^{1}H NMR spectrum of compound **3b**

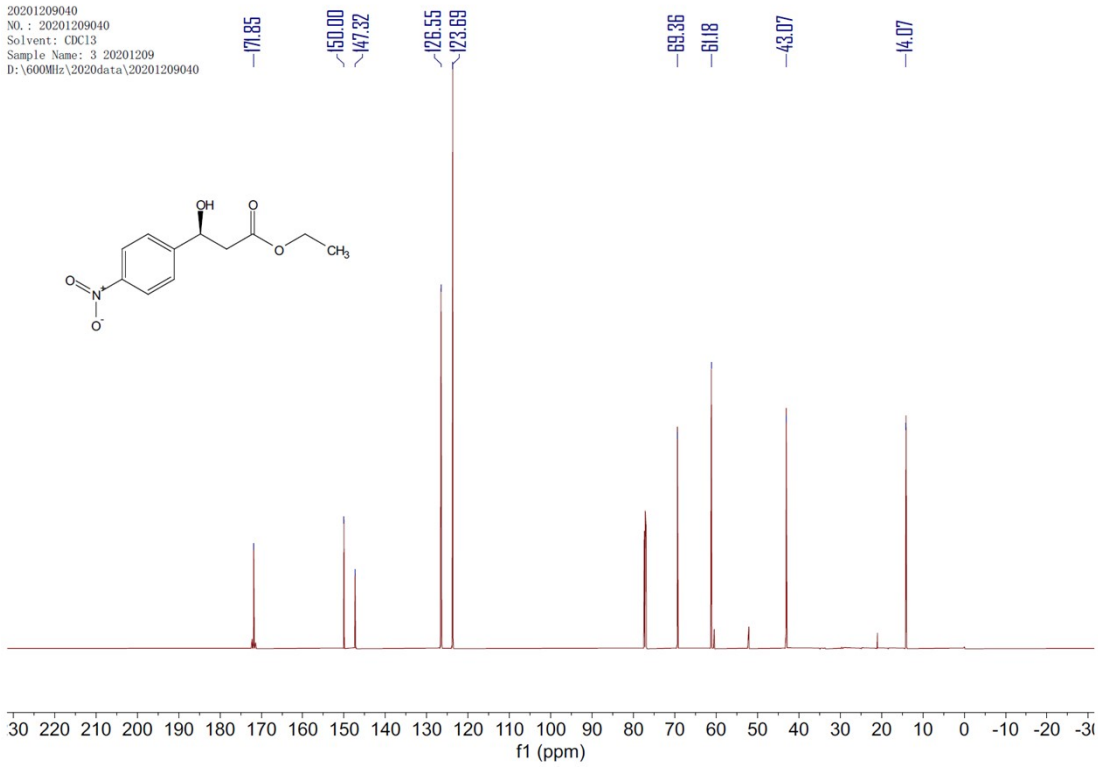

Figure S22. ^{13}C NMR spectrum of compound **3b**

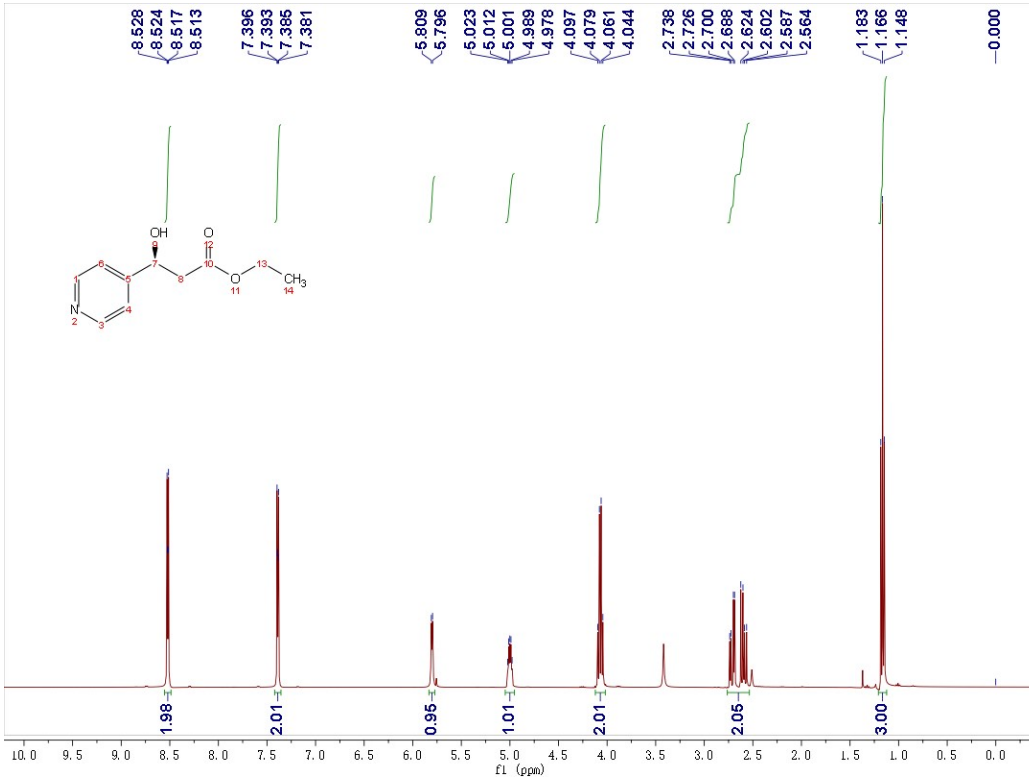

Figure S23. ^{1}H NMR spectrum of compound **4b**

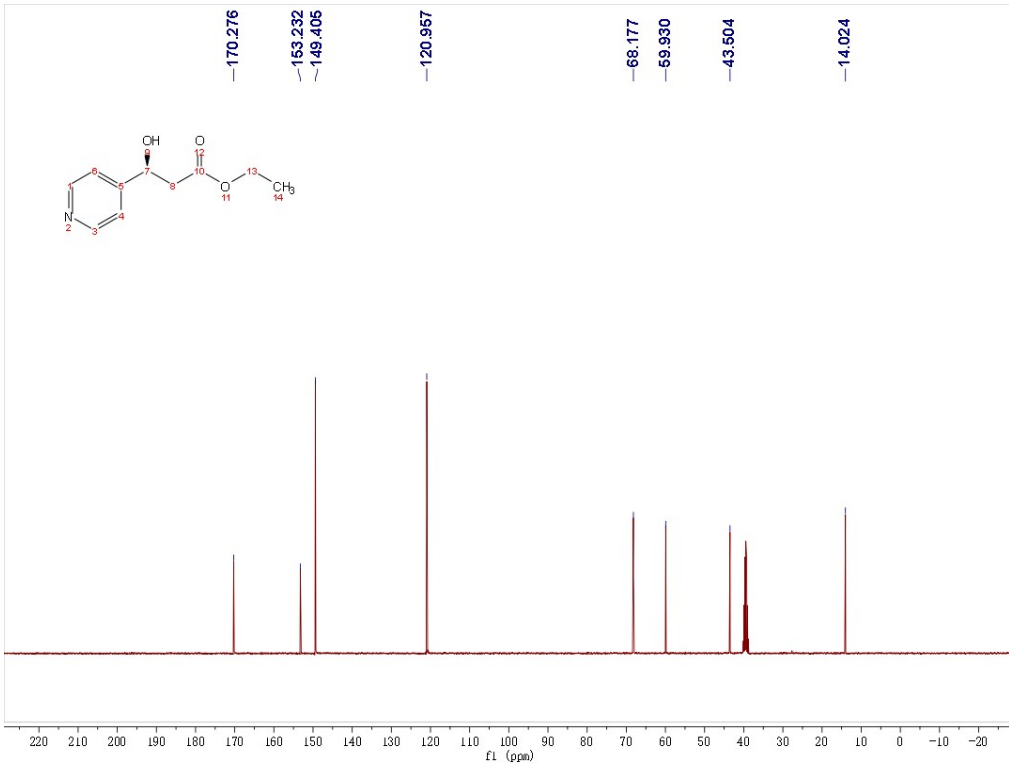

Figure S24. ^{13}C NMR spectrum of compound **4b**

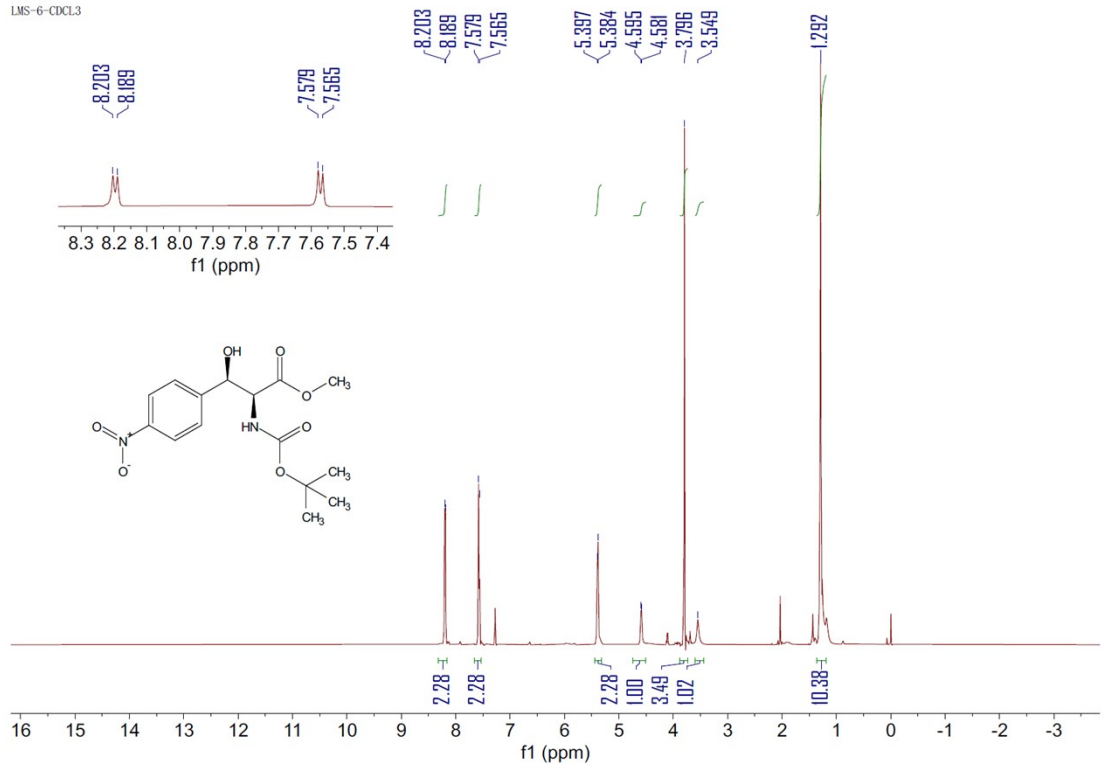

Figure S25. ^{1}H NMR spectrum of compound **5b**

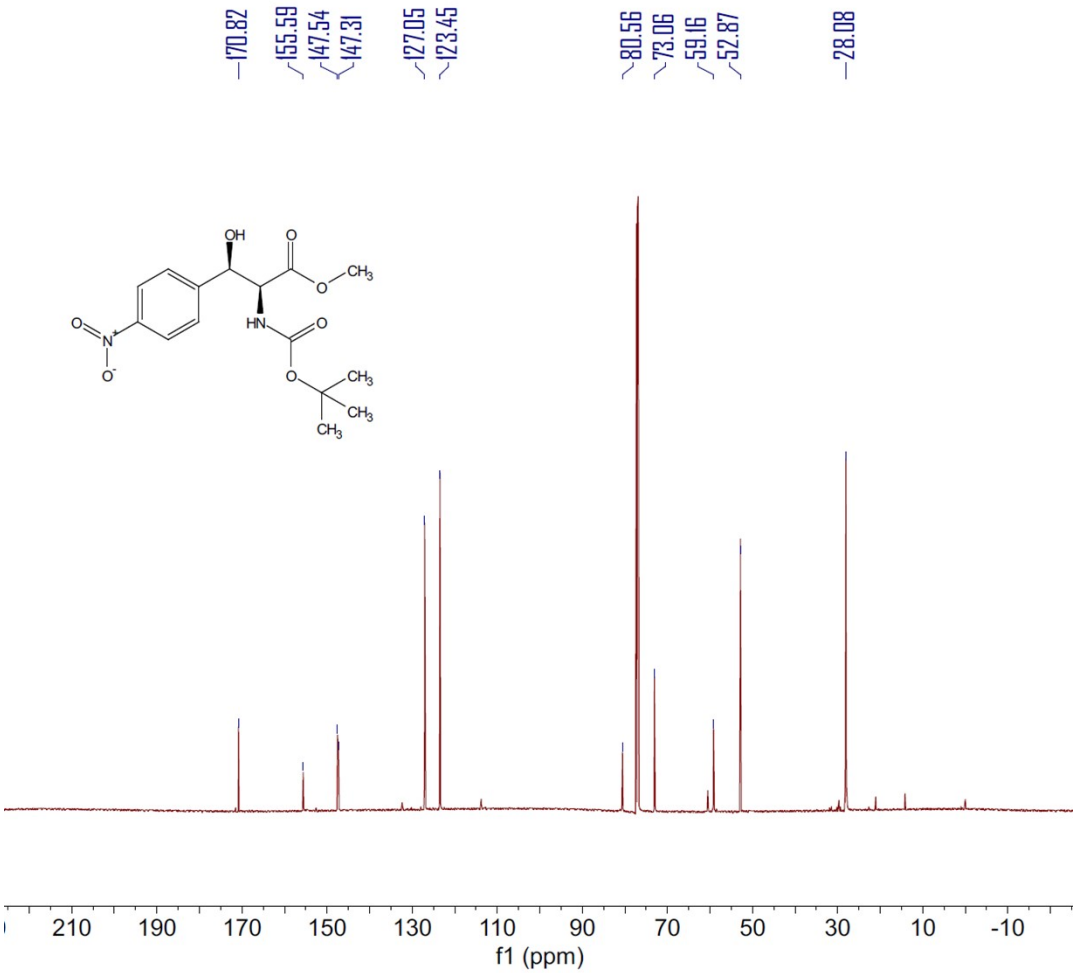

Figure S26. ^{13}C NMR spectrum of compound **5b**

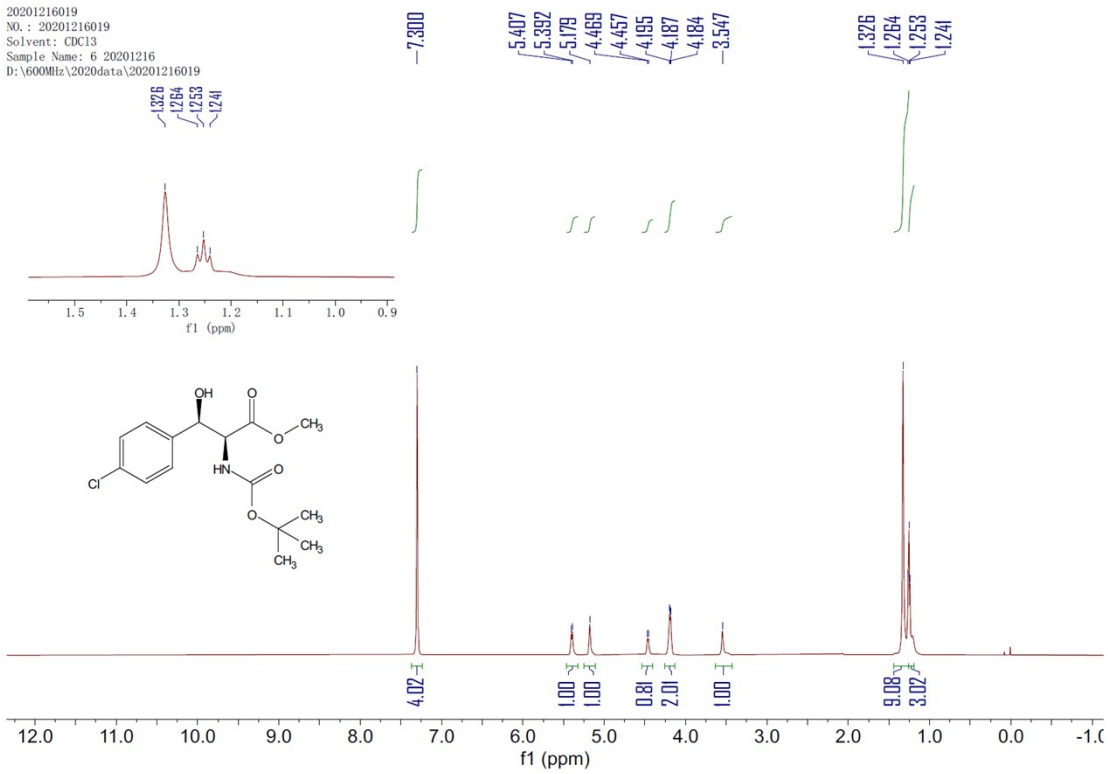

Figure S27. ^{1}H NMR spectrum of compound **6b**

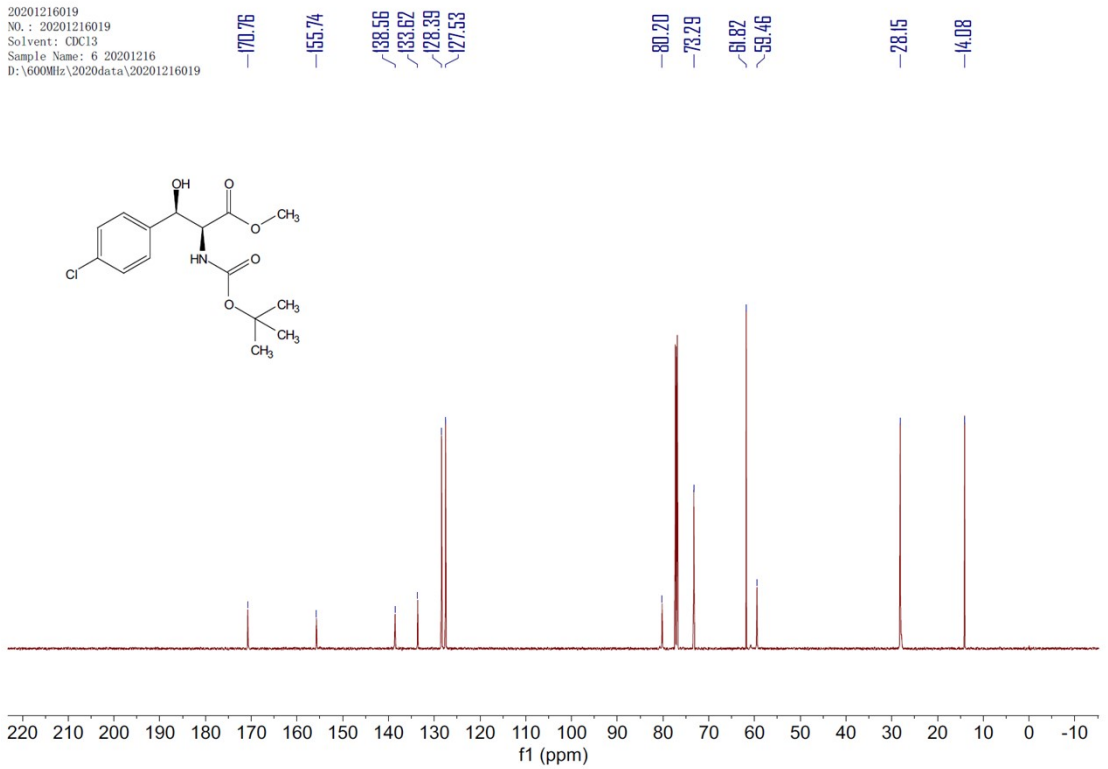

Figure S28. ^{13}C NMR spectrum of compound **6b**

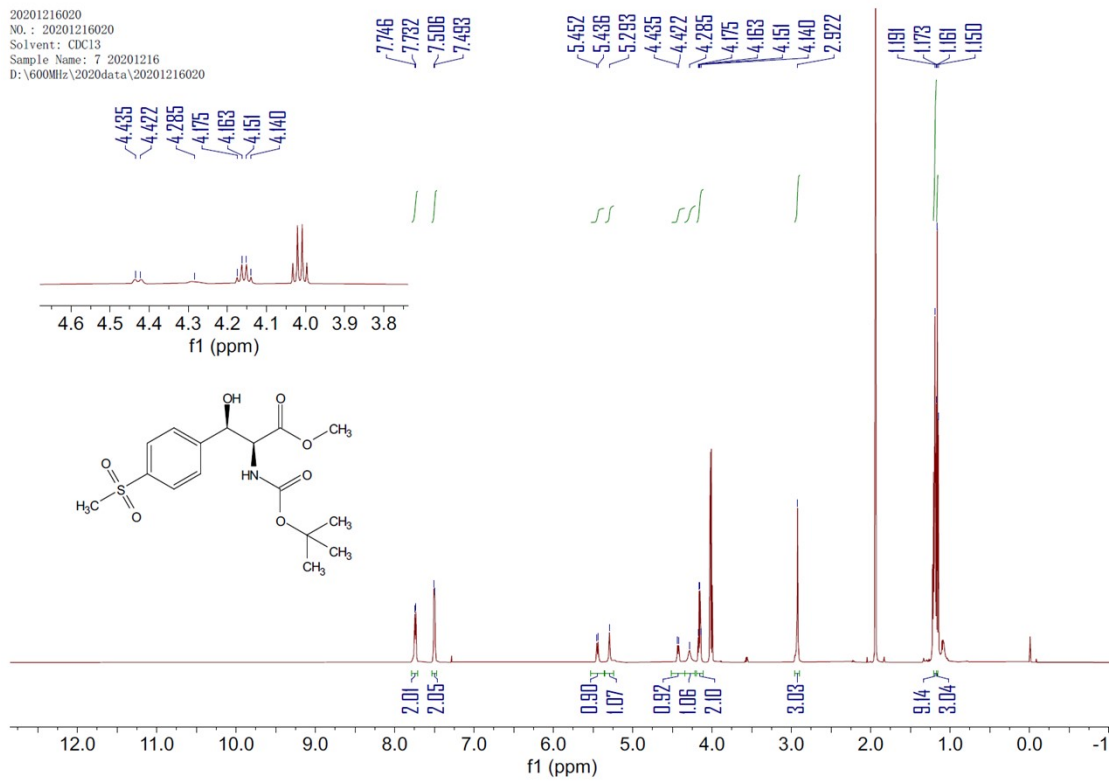

Figure S29. [1]H NMR spectrum of compound **7b**

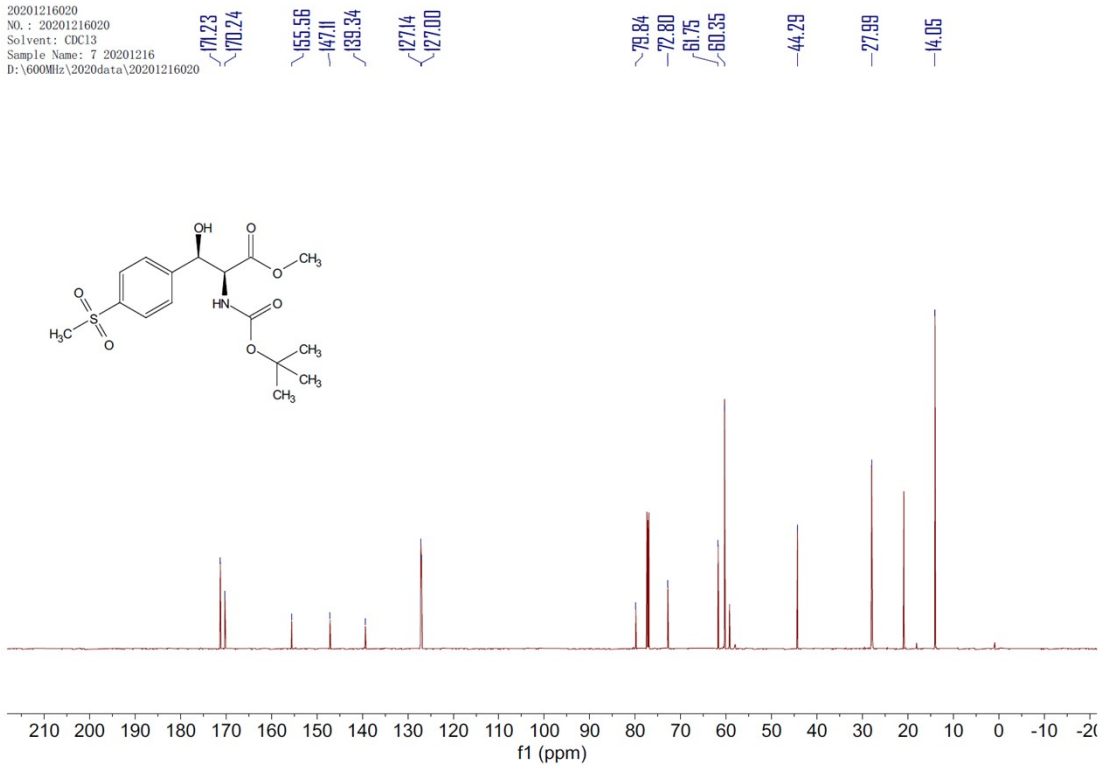

Figure S30. [13]C NMR spectrum of compound **7b**

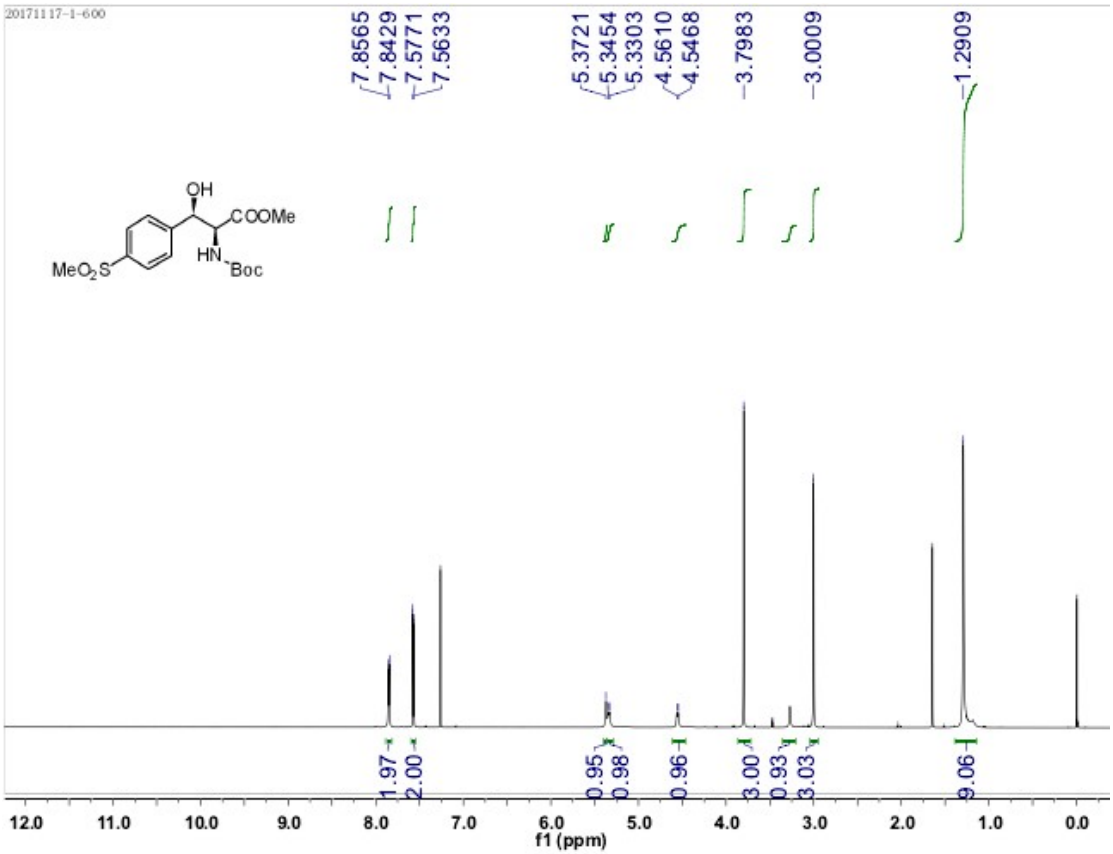

Figure S31. [1]H NMR spectrum of compound **8b**

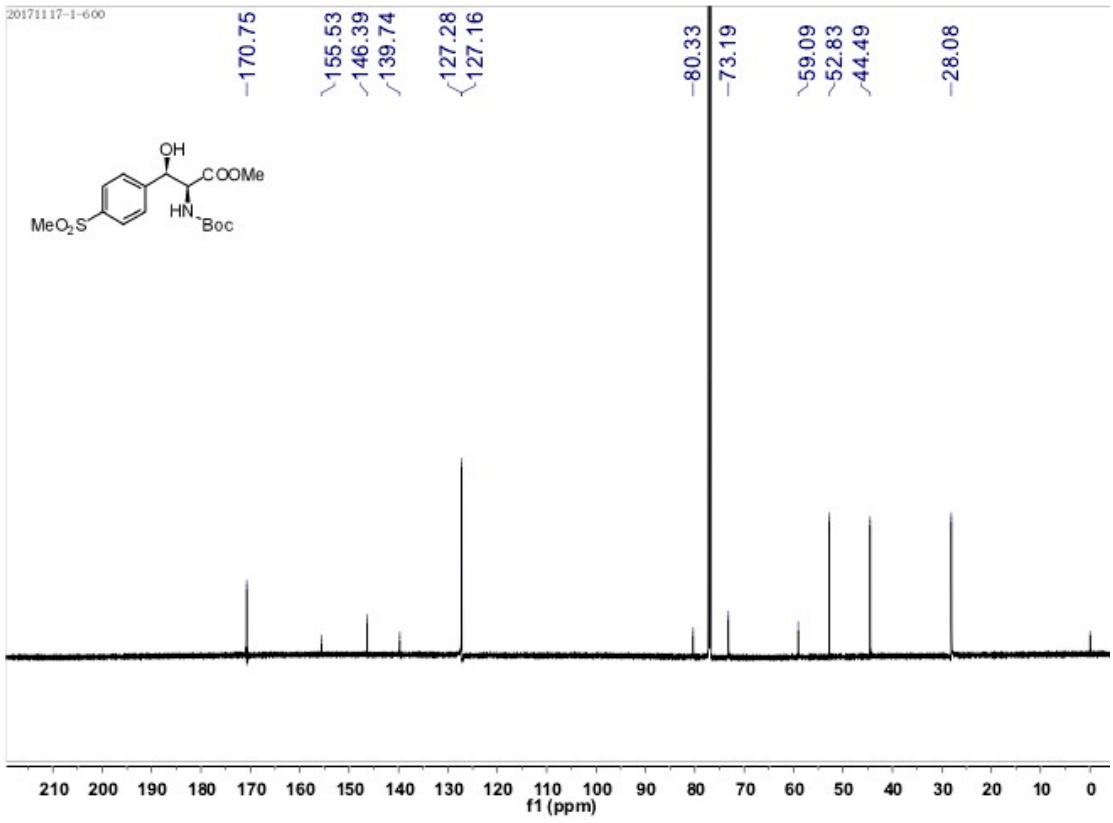

Figure S32. [13]C NMR spectrum of compound **8b**

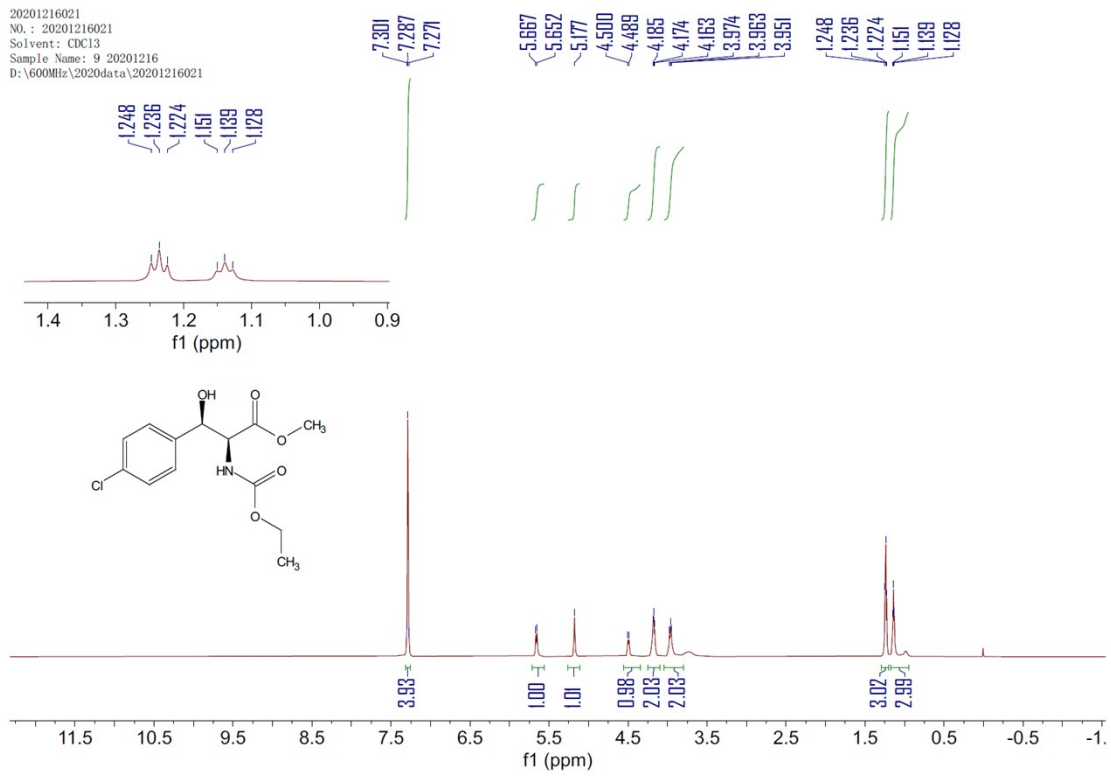

Figure S33. [1]H NMR spectrum of compound **9b**

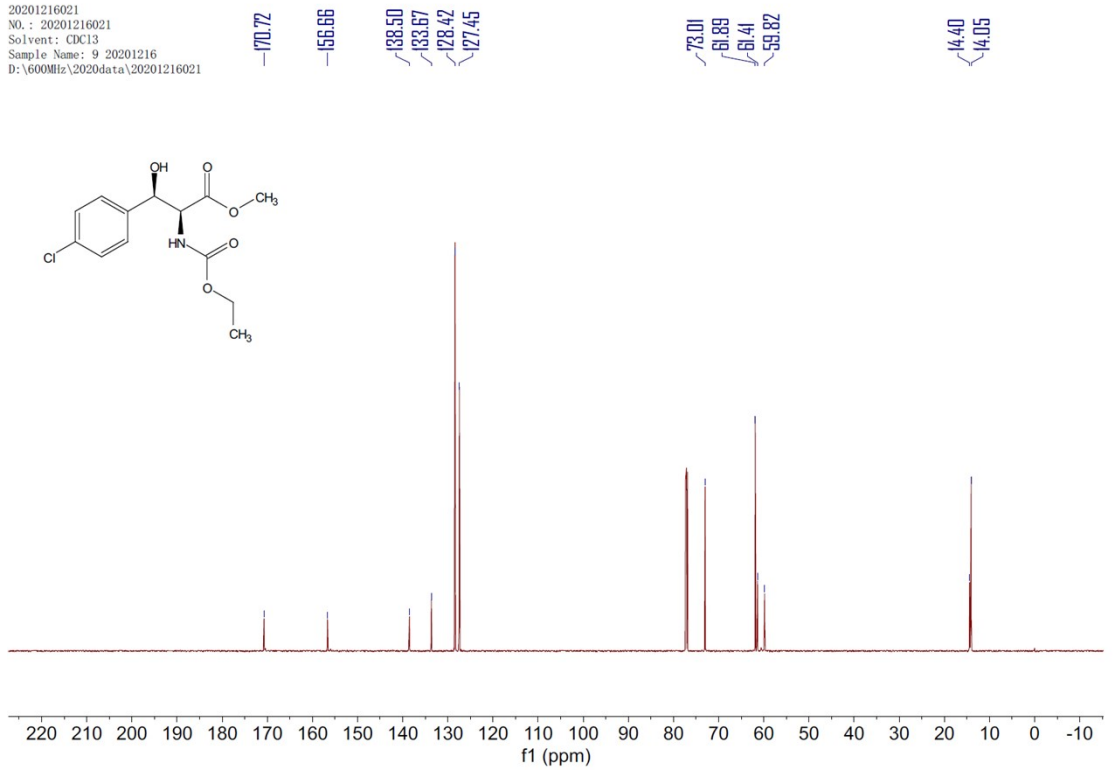

Figure S34. [13]C NMR spectrum of compound **9b**

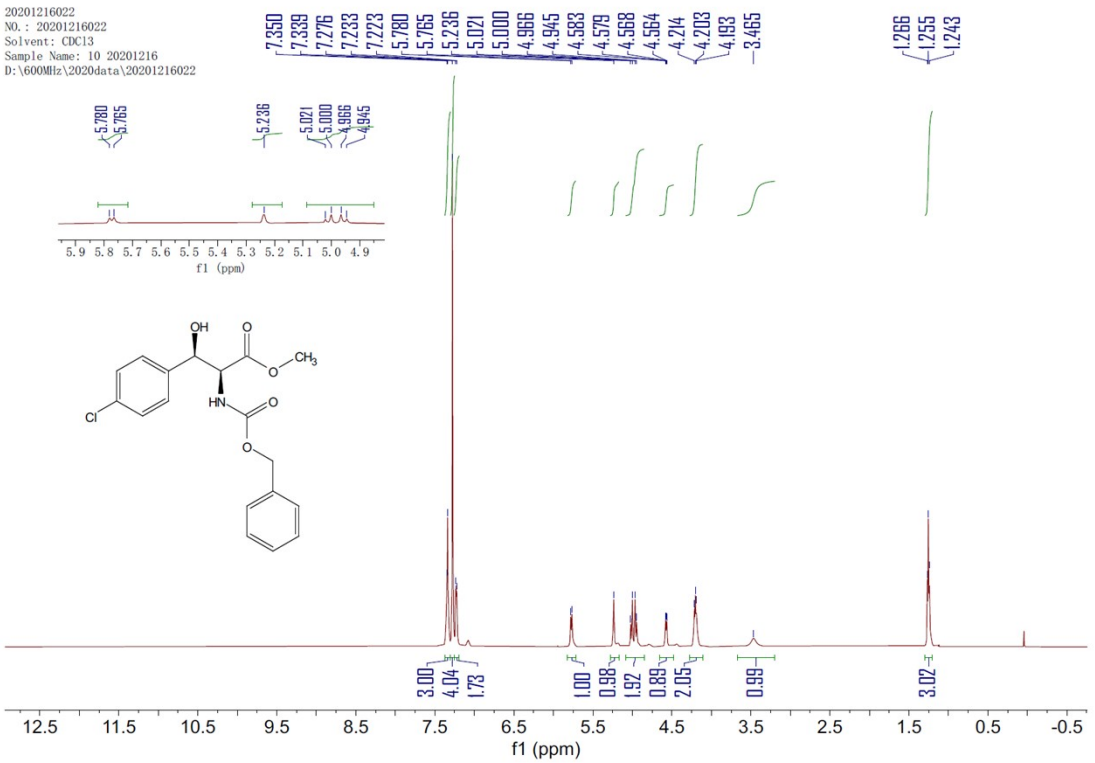

Figure S35. [1]H NMR spectrum of compound **10b**

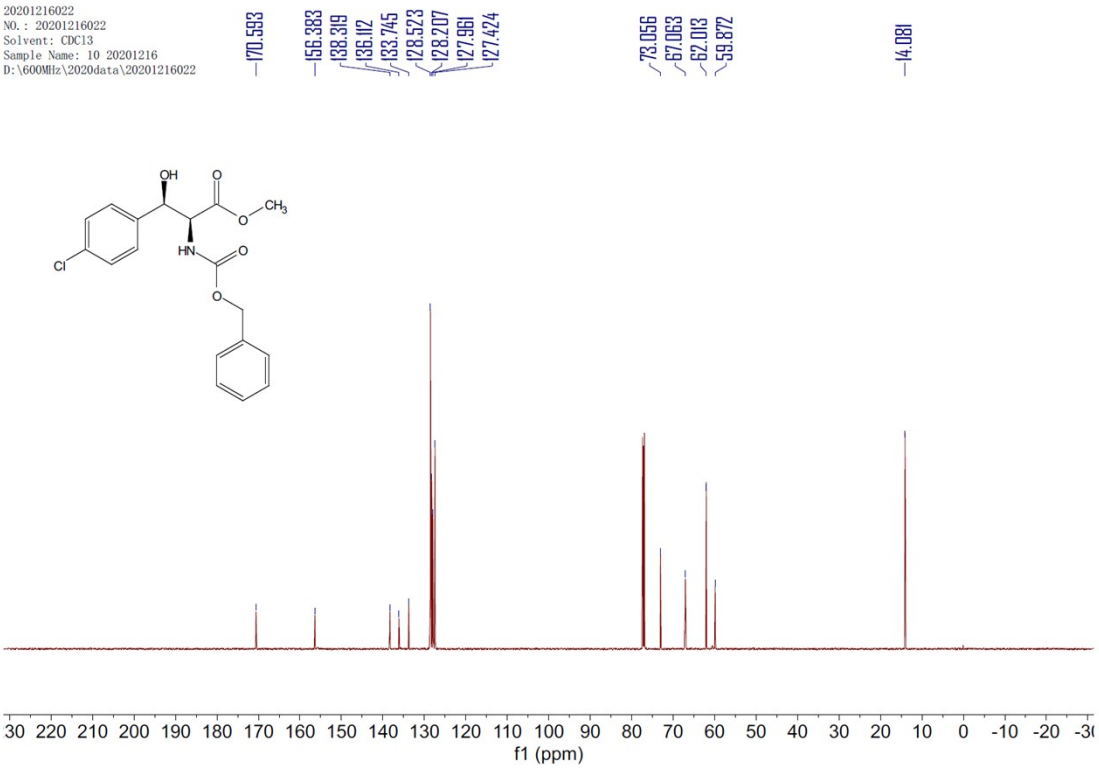

Figure S36. [13]C NMR spectrum of compound **10b**

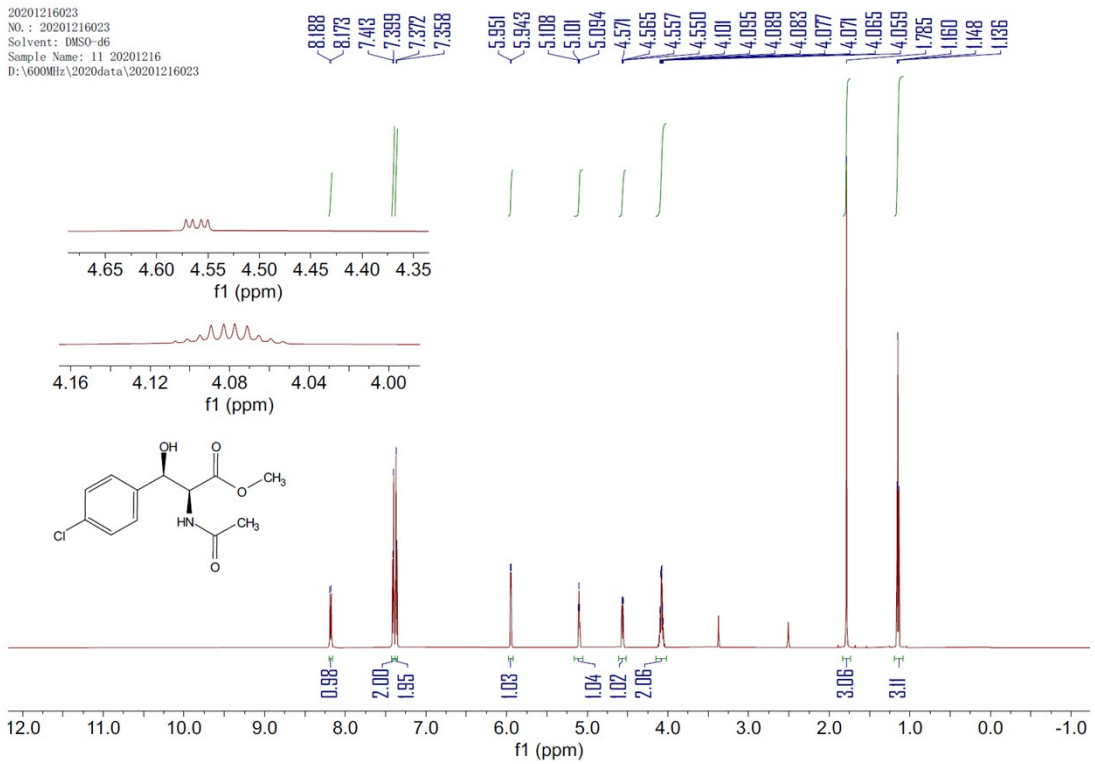

Figure S37. [1]H NMR spectrum of compound **11b**

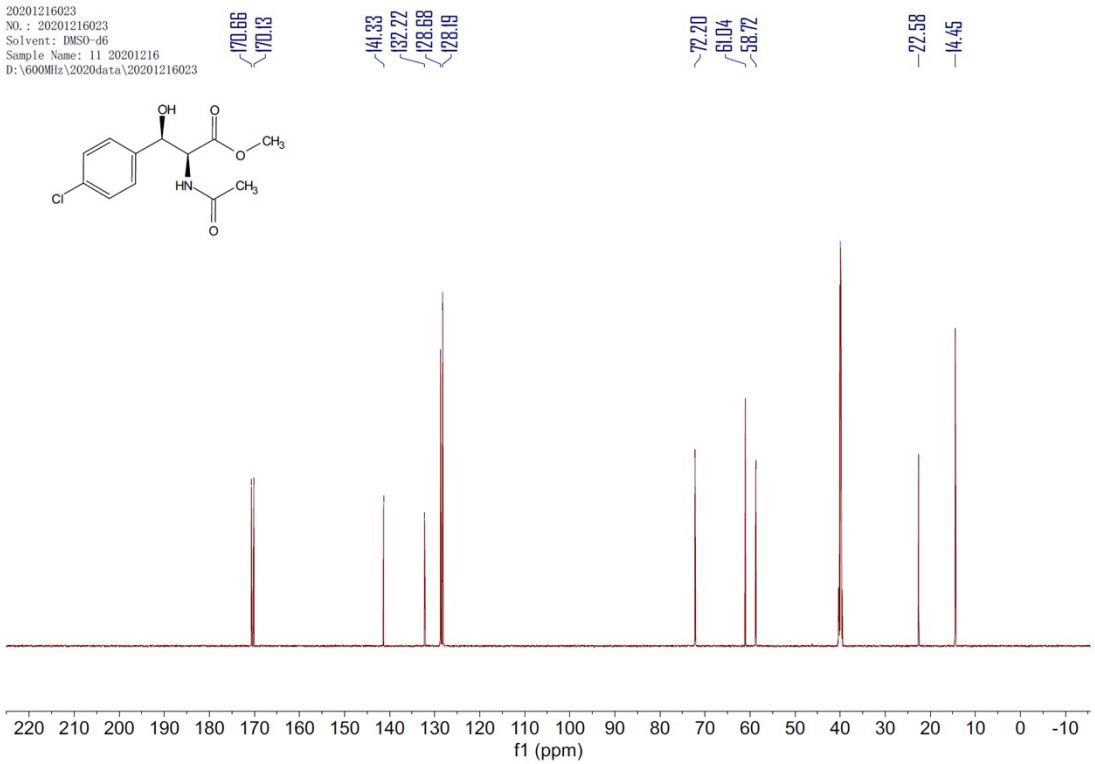

Figure S38. [13]C NMR spectrum of compound **11b**

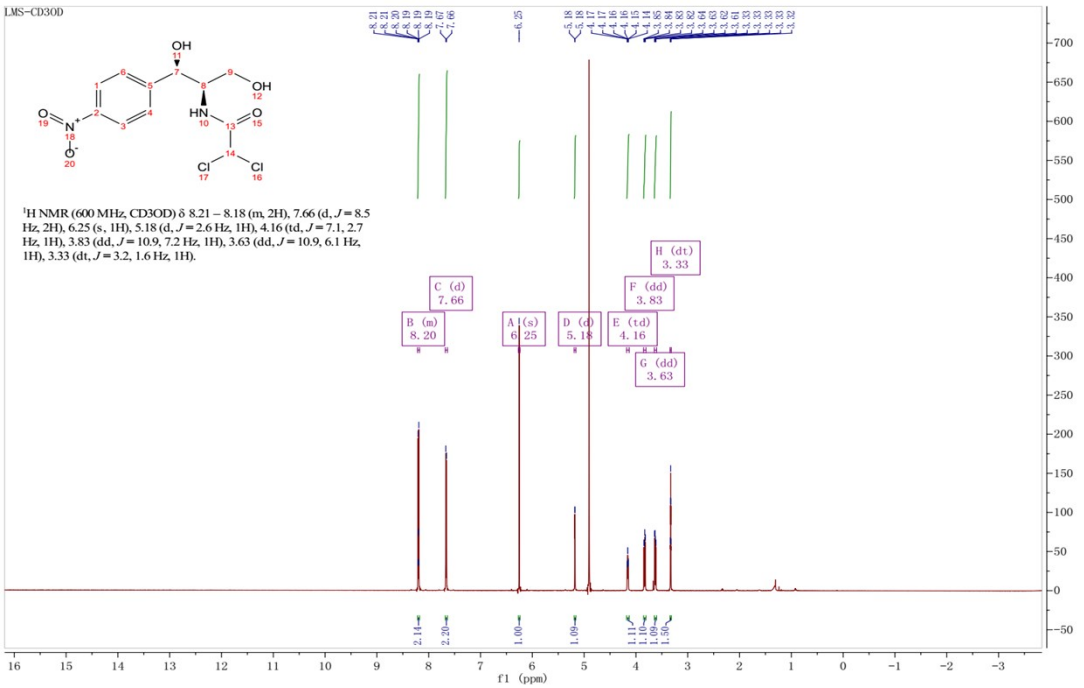

Figure S39. ^{1}H NMR spectrum of chloramphenicol **17**

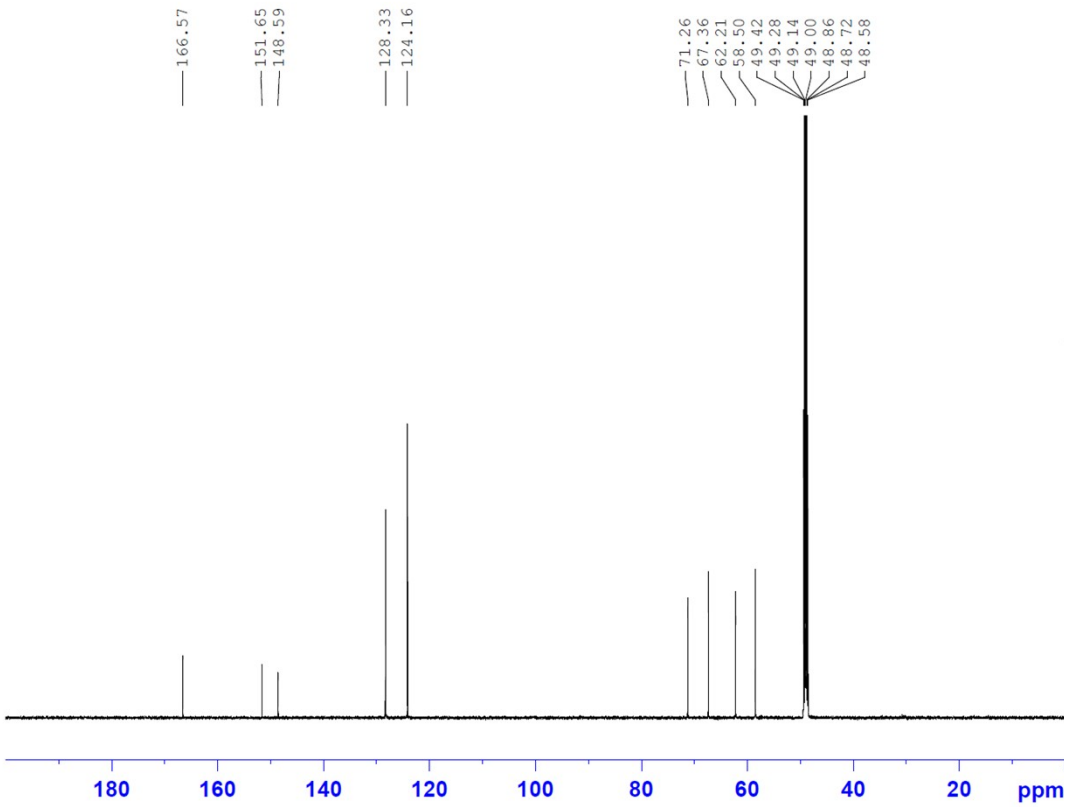

Figure S40. ^{13}C NMR spectrum of chloramphenicol **17**

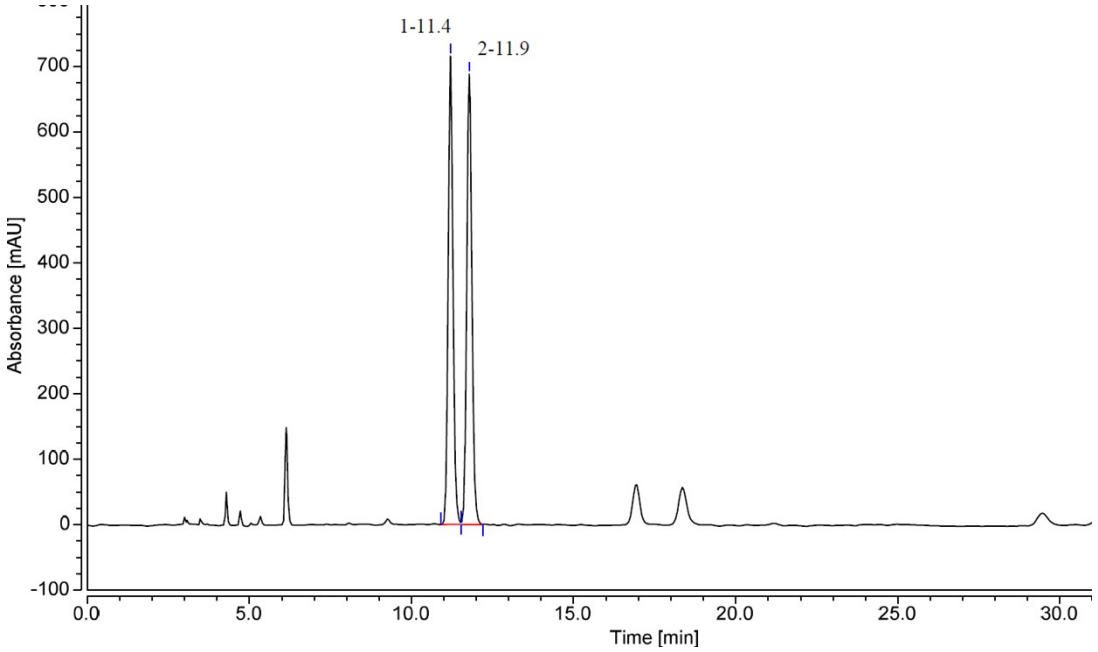

Figure S41. Chiral HPLC chromatogram of compound rac-1

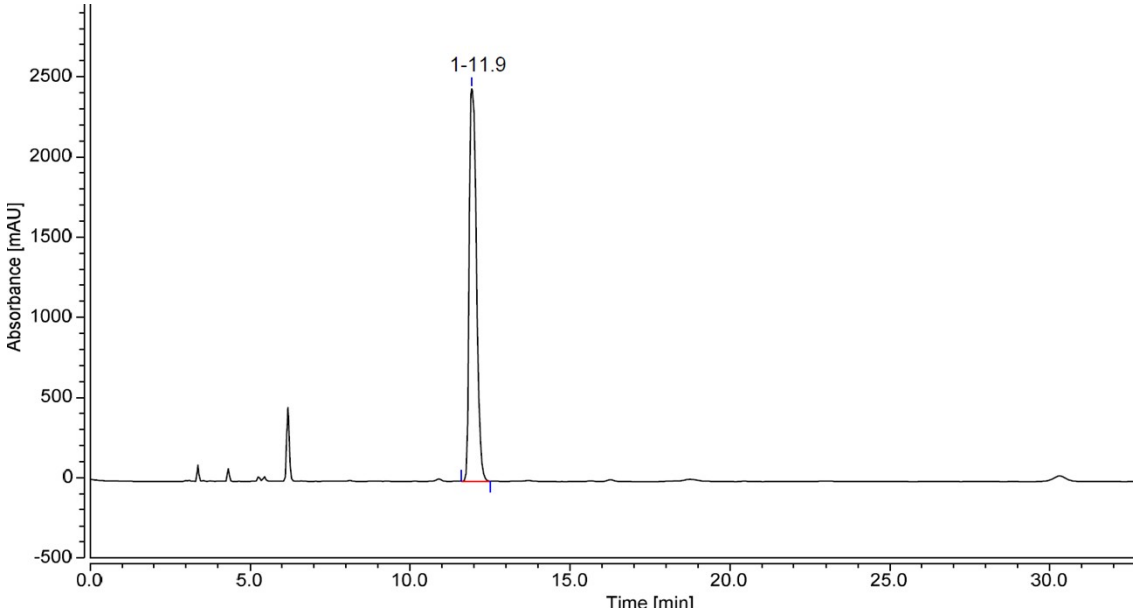

Figure S42. Chiral HPLC chromatogram of compound **1b**

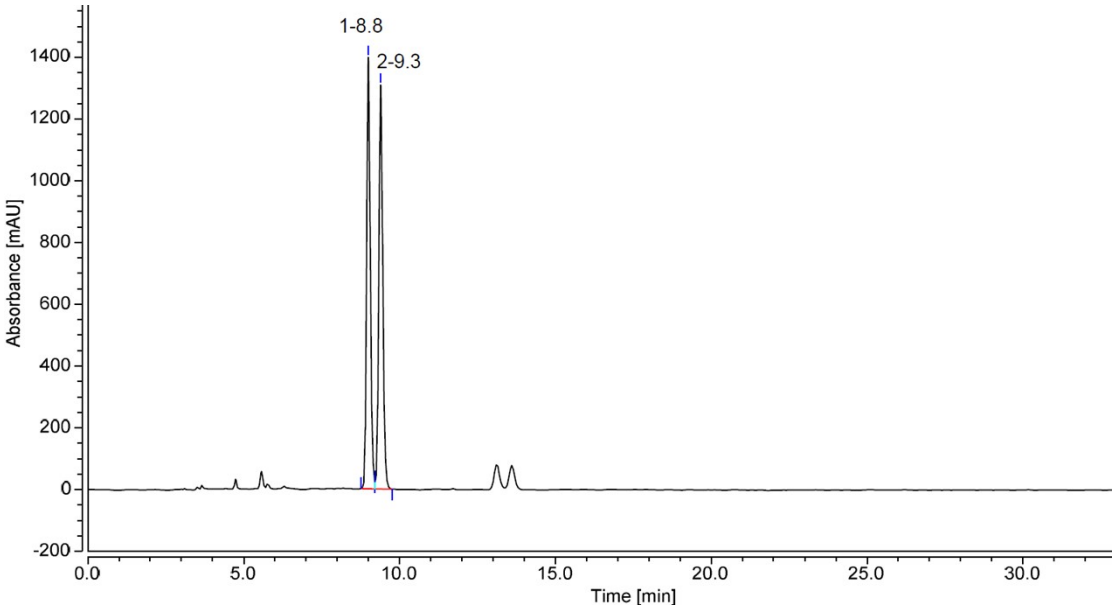

Figure S43. Chiral HPLC chromatogram of compound rac-2

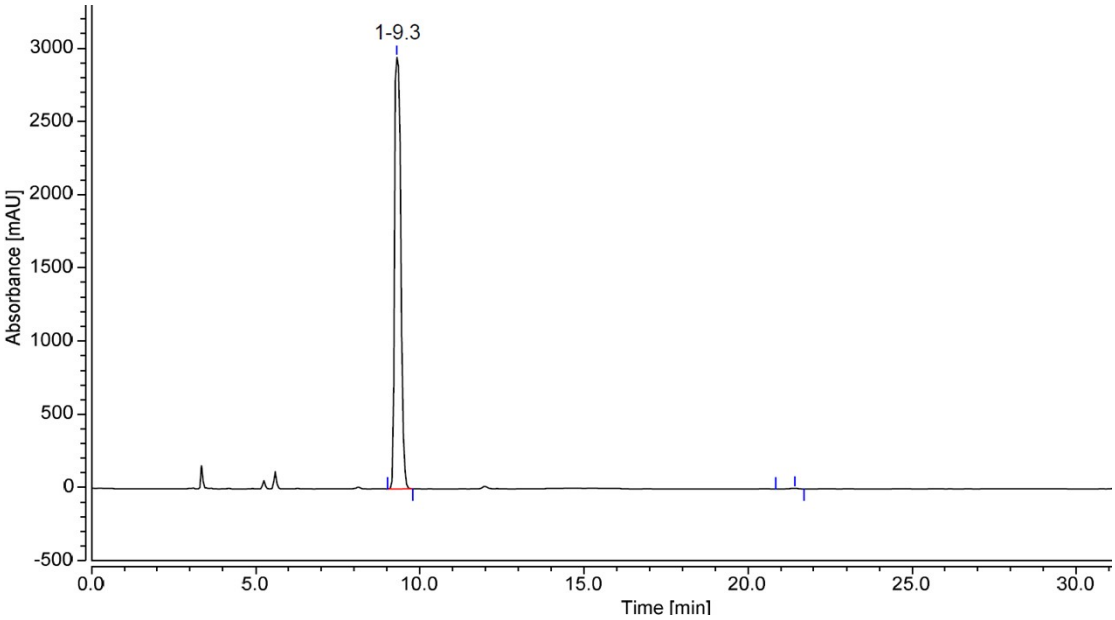

Figure S44. Chiral HPLC chromatogram of compound 2**b**

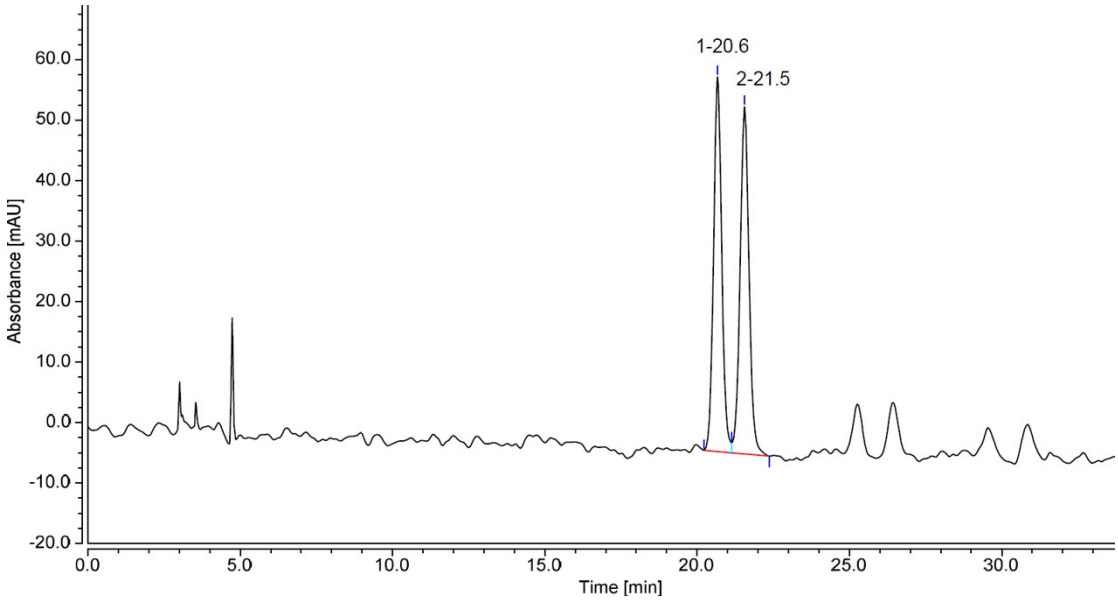

Figure S45. Chiral HPLC chromatogram of compound rac-3

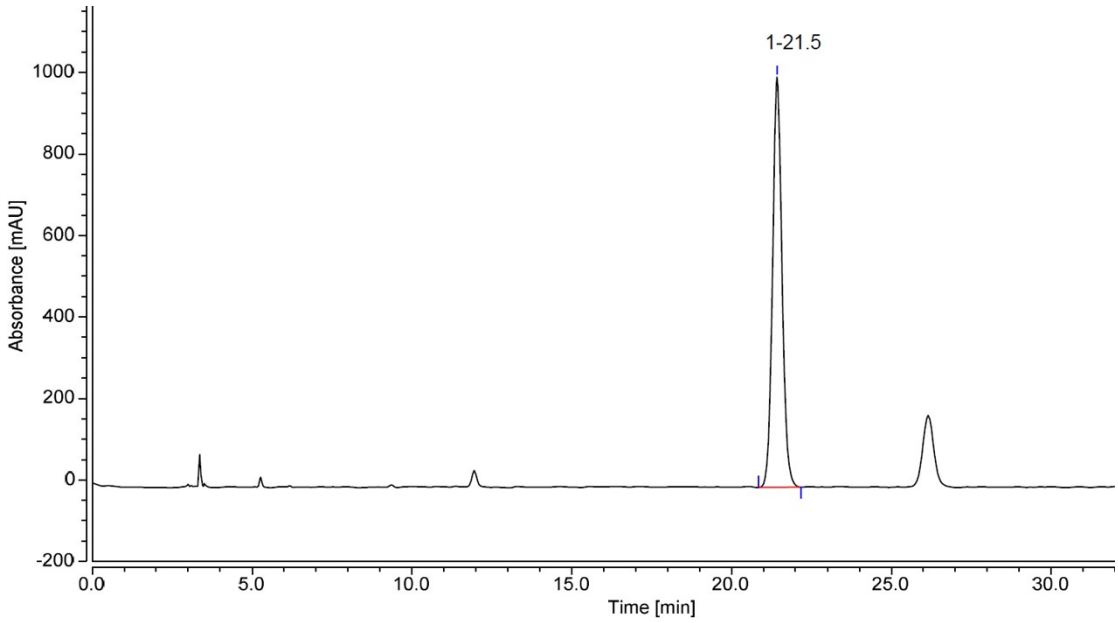

Figure S46. Chiral HPLC chromatogram of compound 3**b**

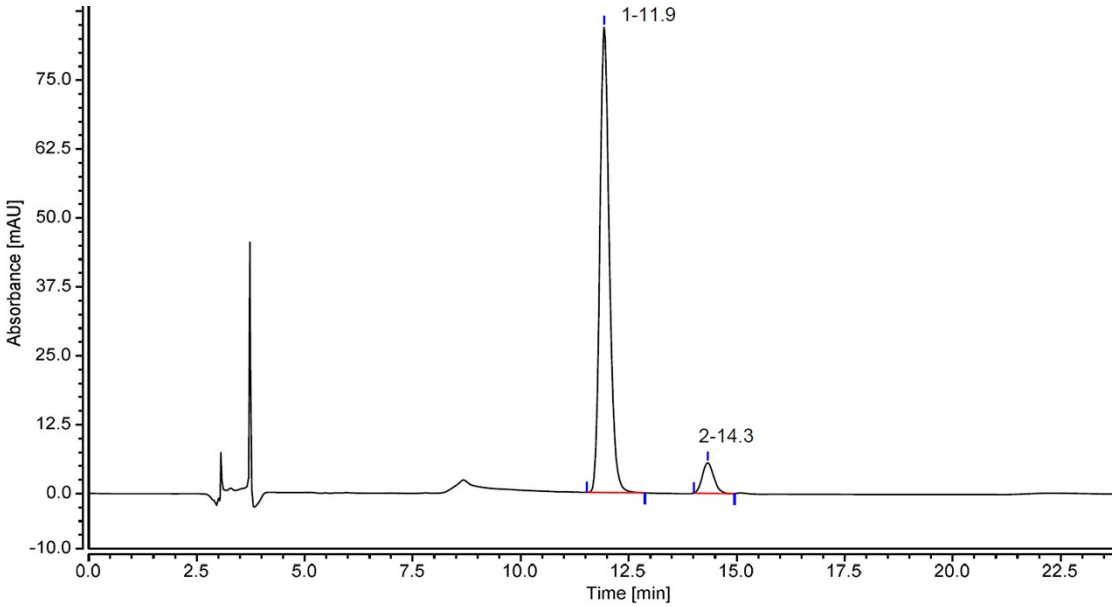

Figure S47. Chiral HPLC chromatogram of compound rac-4

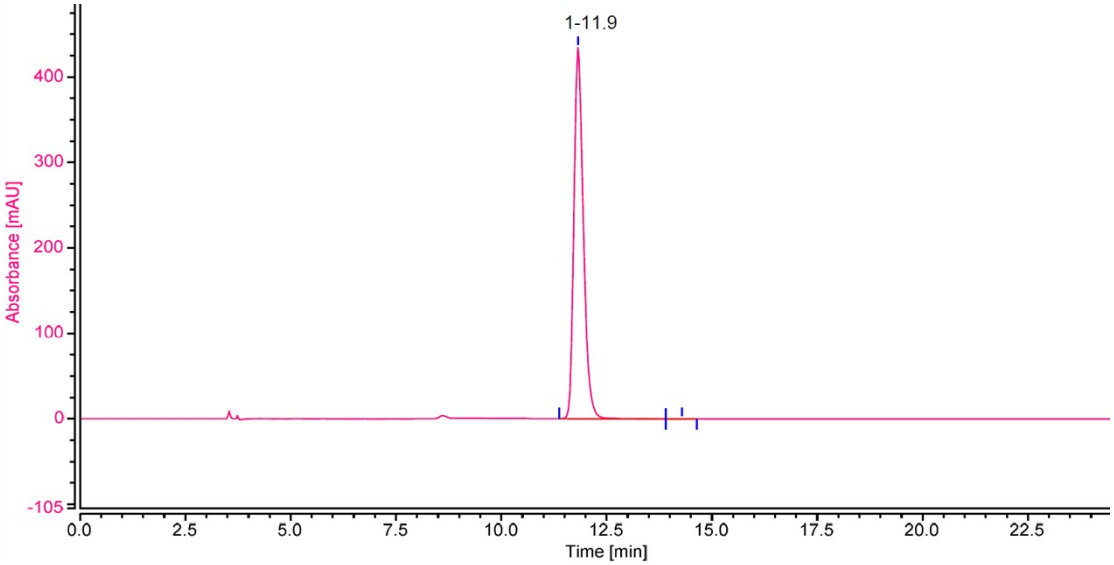

Figure S48. Chiral HPLC chromatogram of compound 4**b**

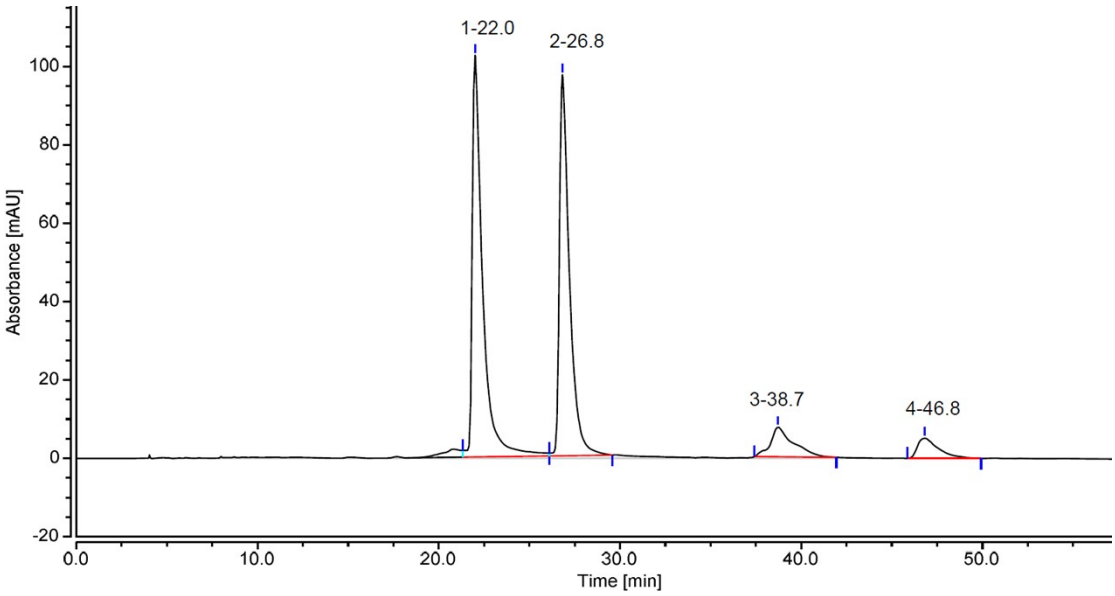

Figure S49. Chiral HPLC chromatogram of compound rac-5

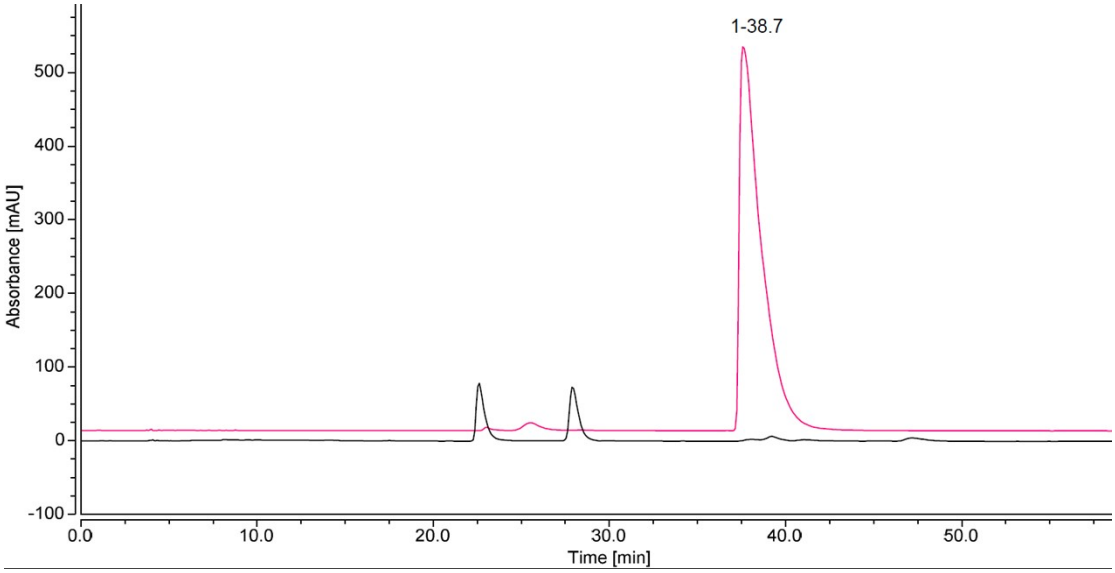

Figure S50. Chiral HPLC chromatogram of compound 5**b**

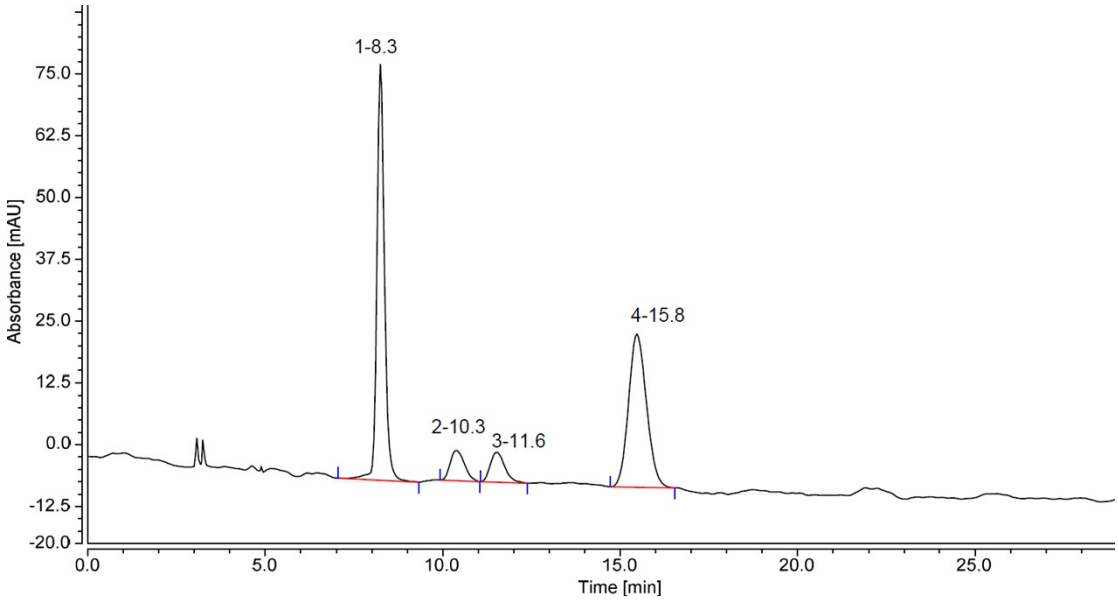

Figure S51. Chiral HPLC chromatogram of compound rac-6

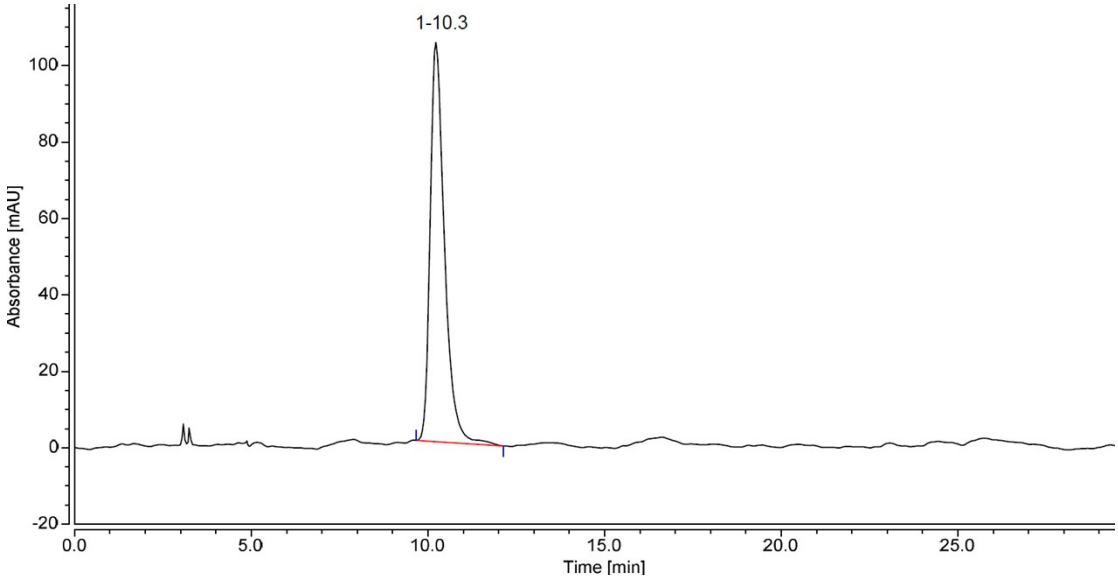

Figure S52. Chiral HPLC chromatogram of compound 6**b**

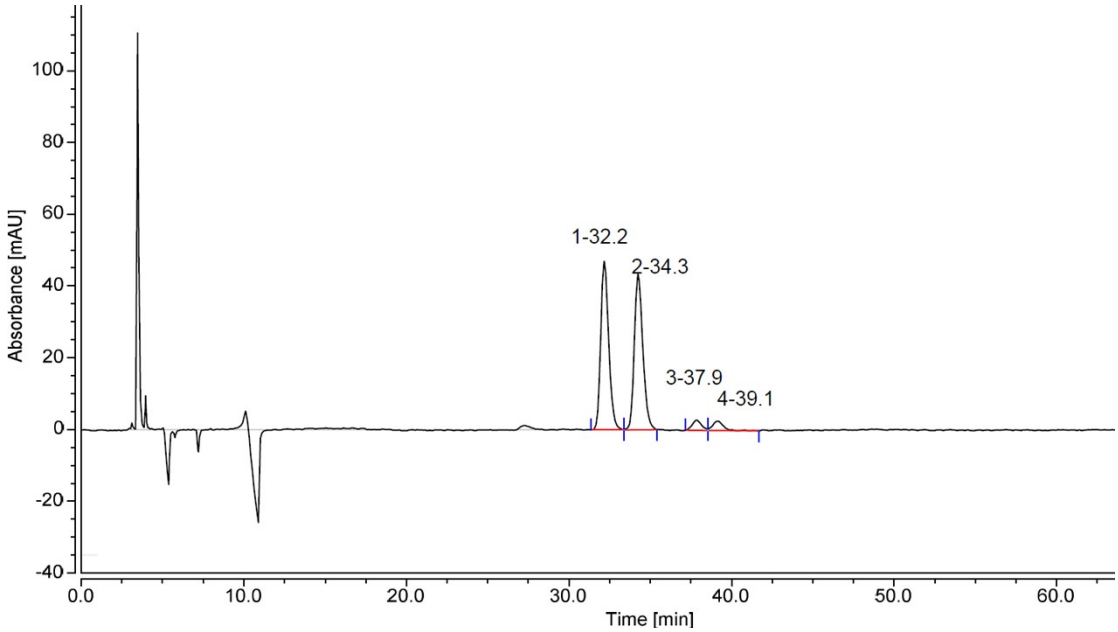

Figure S53. Chiral HPLC chromatogram of compound rac-7

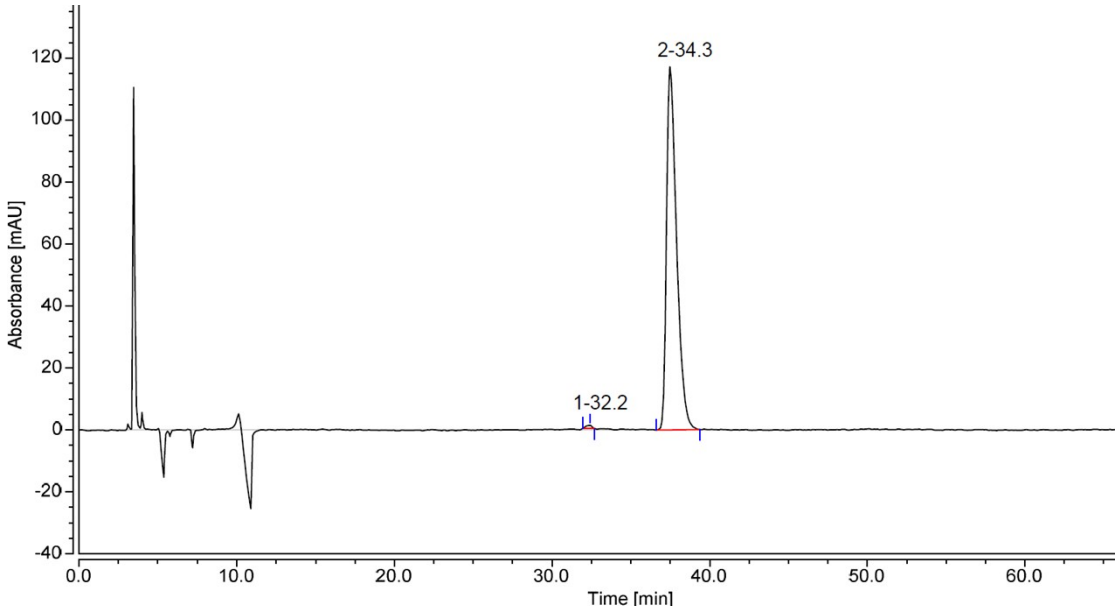

Figure S54. Chiral HPLC chromatogram of compound 7**b**

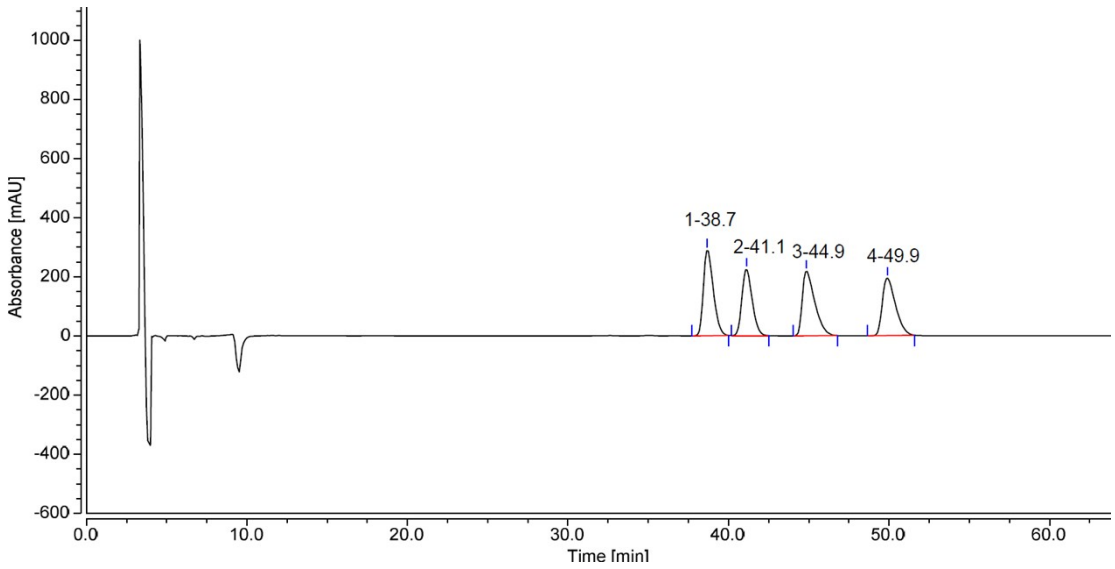

Figure S55. Chiral HPLC chromatogram of compound rac-8

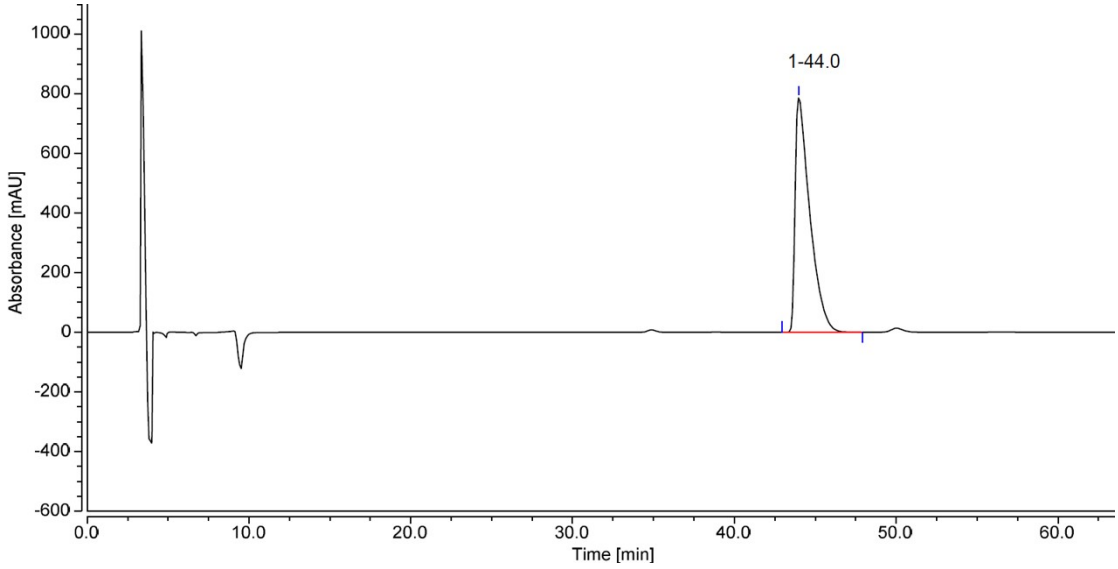

Figure S56. Chiral HPLC chromatogram of compound **8b**

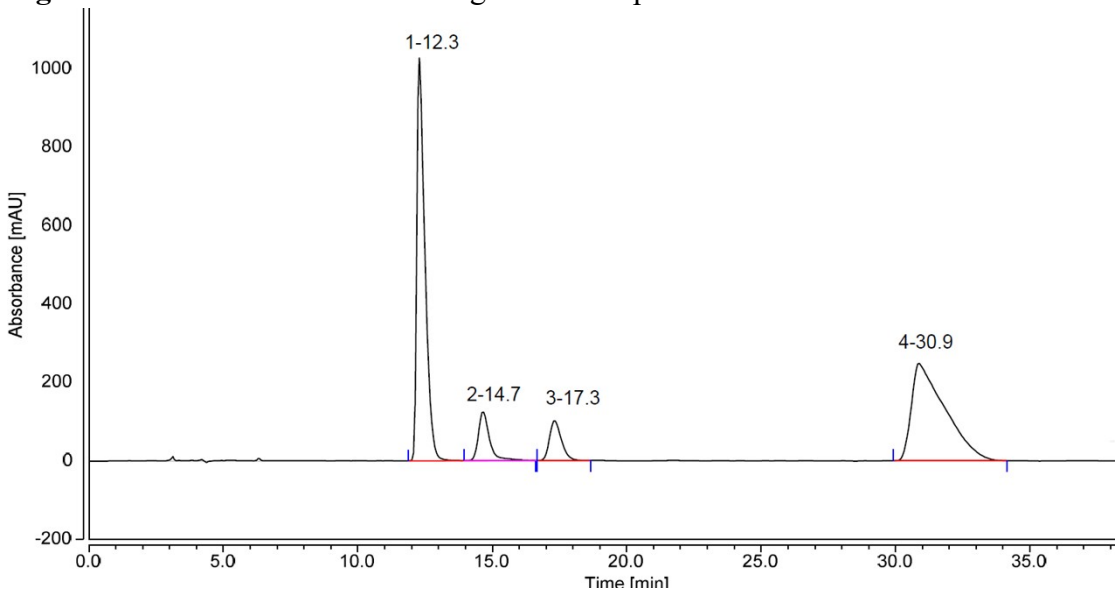

Figure S57. Chiral HPLC chromatogram of compound rac-9

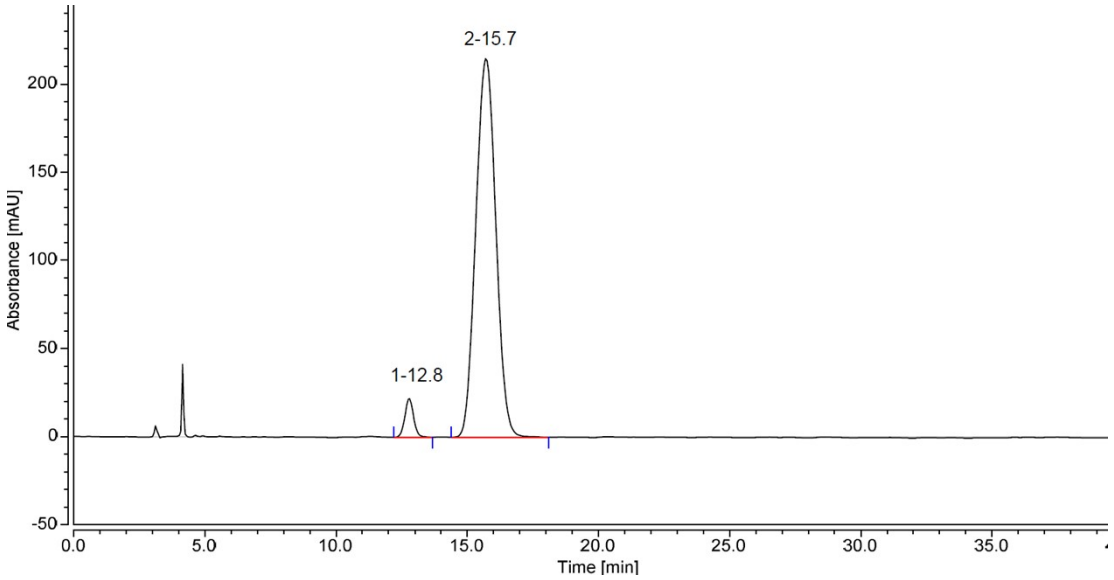

Figure S58. Chiral HPLC chromatogram of compound **9b**

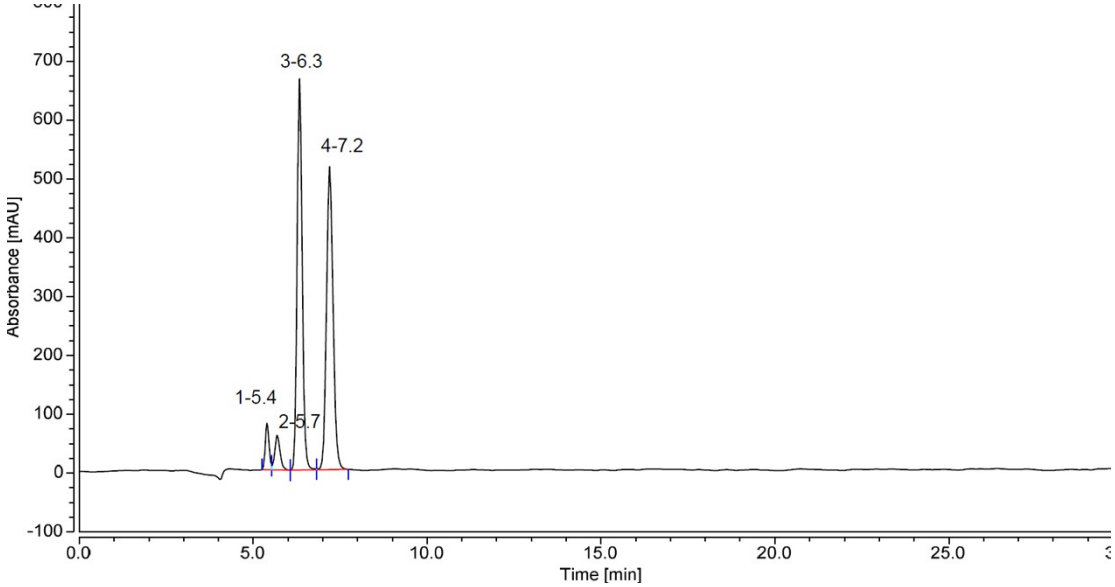

Figure S59. Chiral HPLC chromatogram of compound rac-10

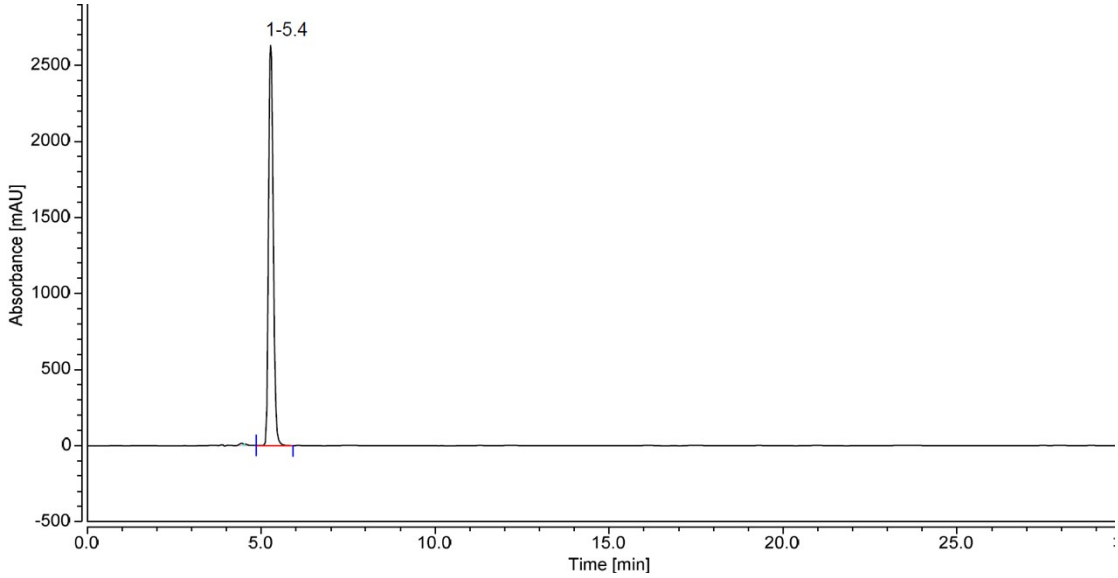

Figure S60. Chiral HPLC chromatogram of compound **10b**

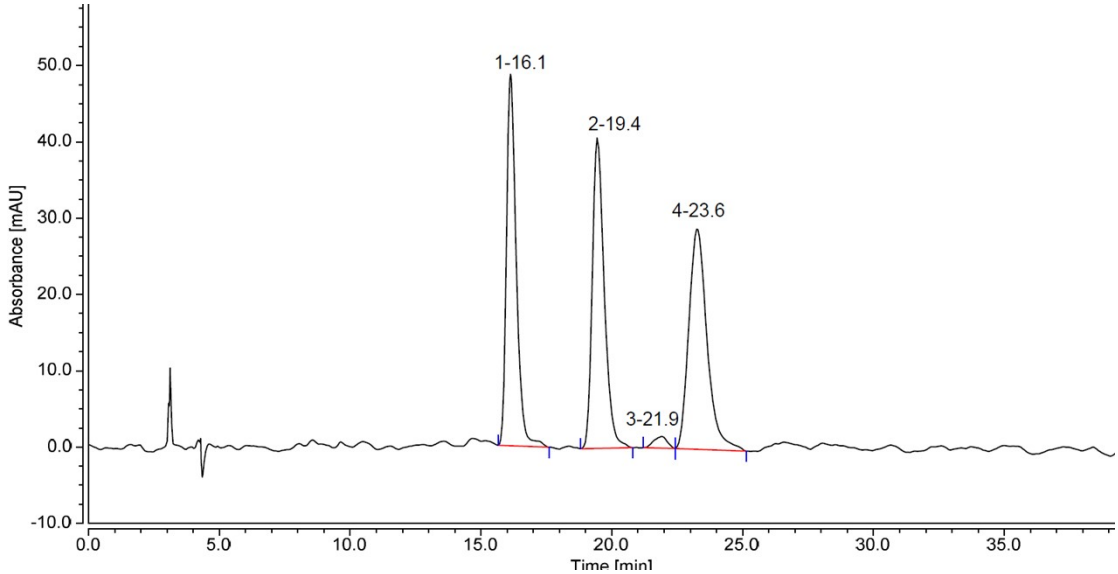

Figure S61. Chiral HPLC chromatogram of compound rac-11

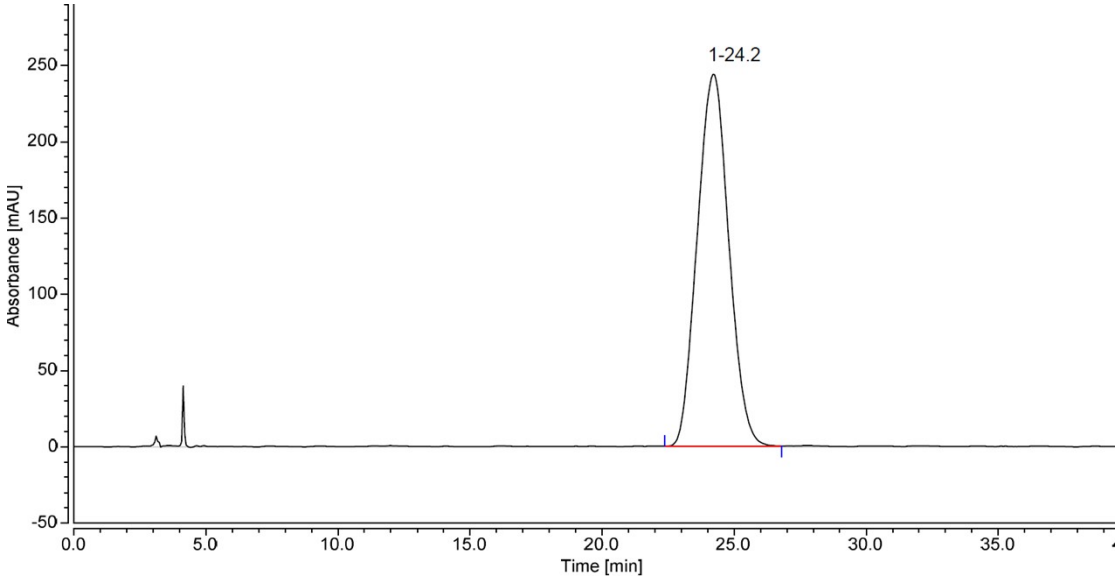

Figure S62. Chiral HPLC chromatogram of compound **11b**

1. Zou, J.; Ni, G.; Tang, J.; Yu, J.; Jiang, L.; Ju, D.; Zhang, F.; Chen, S., Asymmetric Synthesis of Florfenicol by Dynamic Reductive Kinetic Resolution with Ketoreductases. *Eur. J. Org. Chem.* **2018,** *2018* (36), 5044-5053.